Accepted Manuscript

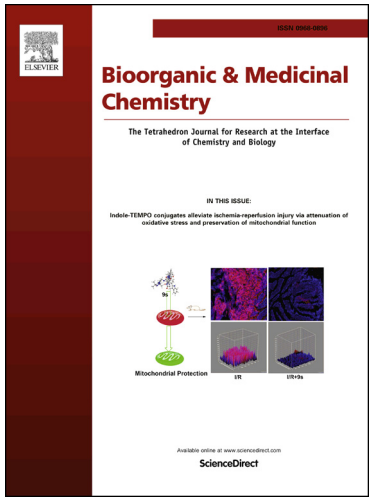

Design, synthesis and biological evaluation of 3,4-dihydro-2(1*H*)-quinoline-*O*-alkylamine derivatives as new multipotent cholinesterase/monoamine oxidase inhibitors for the treatment of Alzheimer's disease

Zhipei Sang, Wanli Pan, Keren Wang, Qinge Ma, Lintao Yu, Wenmin Liu

PII: S0968-0896(17)30013-5
DOI: http://dx.doi.org/10.1016/j.bmc.2017.03.070
Reference: BMC 13669

To appear in: *Bioorganic & Medicinal Chemistry*

Received Date: 4 January 2017
Accepted Date: 22 March 2017

Please cite this article as: Sang, Z., Pan, W., Wang, K., Ma, Q., Yu, L., Liu, W., Design, synthesis and biological evaluation of 3,4-dihydro-2(1*H*)-quinoline-*O*-alkylamine derivatives as new multipotent cholinesterase/monoamine oxidase inhibitors for the treatment of Alzheimer's disease, *Bioorganic & Medicinal Chemistry* (2017), doi: http://dx.doi.org/10.1016/j.bmc.2017.03.070

Design, synthesis and biological evaluation of 3,4-dihydro-2(1*H*)-quinoline-*O*-alkylamine derivatives as new multipotent cholinesterase/monoamine oxidase inhibitors for the treatment of Alzheimer's disease

Zhipei Sang[a, *], Wanli Pan[a], Keren Wang[b], Qinge Ma[a] , Lintao Yu[a], Wenmin Liu[a, *].

[a]College of Chemistry and Pharmaceutical Engineering, Nanyang Normal University, Nanyang, 473061, China

[b]Nanyang Normal University Hospital, Nanyang Normal University, Nanyang, 473061, China

Abbreviations: AD, Alzheimer's disease; AChE, acetylcholinesterase; BuChE, butyrylcholinesterase; ACh, acetylcholine; MAO, monoamine oxidase; MTDLs, multi-target-directed ligands; *Ee*AChE, *Electrophorus electricus* AChE; eqBuChE, *equine serum* BuChE; SD, standard deviation; PDB, Protein Data Bank; CAS, catalytic active site; PAS, peripheral anionic site; PAMPA-BBB, parallel artificial membrane assay for the blood- brain barrier; TPSA, topological polar surface area; ADME, absorption, distribution, metabolism, and excretion; HPLC, high-performance liquid chromatography; PBL, Porcine brain lipid; ATC, acetylthiocholine chloride; BTC, butyrylthiocholine chloride.

* *Corresponding Author*.

E-mail: sangzhipei@126.com (Zhipei Sang)

E-mail: liuwm1969@163.com (Wenmin Liu)

Abstract

A new family of multitarget molecules able to interact with acetylcholinesterase (AChE) and butyrylcholinesterase (BuChE), as well as with monoamino oxidase (MAO) A and B, has been synthesized. Novel 3,4-dihydro-2(1*H*)-quinoline-*O*-alkylamine derivatives have been designed using a conjunctive approach that combines the **JMC49** and donepezil. The most promising compound **TM-33** showed potent and balance inhibitory activities toward ChE and MAO (eeAChE, eqBuChE, hMAO-A and hMAO-B with IC_{50} values of 0.56 μM, 2.3 μM, 0.3 μM and 1.4 μM, respectively) but low selectivity. Both kinetic analysis of AChE inhibition and molecular modeling study suggested that **TM-33** binds simultaneously to the catalytic active site and peripheral anionic site of AChE. Furthermore, our investigation proved that **TM-33** could cross the blood-brain barrier (BBB) *in vitro*, and abided by Lipinski's rule of five. The results suggest that compound **TM-33**, an interesting multi-targeted active molecule, offers an attractive starting point for further lead optimization in the drug-discovery process against Alzheimer's disease.

Keywords: Alzheimer's disease; 3,4-dihydro-2(1*H*)-quinoline-*O*-alkylamines; AChE inhibitor; BuChE inhibitor; MAO-A inhibitor; MAO-B inhibitor; blood–brain barrier.

1. Introduction

Alzheimer's disease (AD), the most common form of adult onset dementia, is an age-related neurodegenerative disorder characterized by a progressive memory loss, a decline in language skills, and other cognitive impairments.[1] In 2015, there was an estimated 46 million people living with dementia worldwide, the dementia number is estimated to increase to 131.5 million by 2050. Dementia also has a huge economic impact, the total estimated worldwide cost of dementia is US $818 billion, and it will become 2 trillion dollar disease by 2030.[2] Current clinical treatment of AD is mainly focused on the symptomatic aspects. The cholinergic hypothesis of memory dysfunction in AD is the basis for treating this disease.[3] In particular, the main approach in the AD treatment is the improvement of cholinergic neurotransmission by inhibiting acetylcholinesterase (AChE) and butyrylcholinesterase (BuChE).[4] By increasing the levels of acetylcholine (ACh) in the brain through inhibition of these enzymes, it is possible to reducing cognitive decline but cannot prevent, halt, or reverse the progression of the disease.[5]

AD is a complicated disease with different molecular events, the decline in the cholinergic function of the brain results in the loss of memory and cognitive functions which are usually accompanied by behavioral disturbances.[6] Studies showed that serotoninergic and dopaminergic, were also thought to be responsible for the behavioral disturbances observed in patients with AD.[7-9] It suggested that inhibitors of monoamine oxidase (IMAOs) might be also valuable for the treatment of AD. Thus, monoamine oxidase (MAO), the enzyme that catalyzes the oxidative deamination of a variety of biogenic and xenobiotic amines, is also an important target to be considered for the treatment of specific features of this multifactorial disease.[10] MAO exists as two distinct enzymatic isoforms, MAO-A and MAO-B, based on their substrate and inhibitor specificities. Selective inhibitors for MAO-A have been shown to be effective antidepressants, whereas MAO-B inhibitors, although apparently devoid of antidepressant action, are useful in the treatment of Parkinson's disease.[11] Moreover, AD patients commonly present depressive symptoms that have even considered as a risk factor for the development of the disease.[12] Increased MAO-B levels due to

enhance astrogliosis in the brain of AD patients have also been reported.[13] Overall, these observations revealed that dual inhibition of MAO-A and MAO-B, rather than MAO-B alone, may be of value for AD therapy.[14]

Given that the complexity of AD and the involvement of multi-systems in its progression, one single drug that acts on a specific target to produce the desired clinical effects might not be suitable for the complex nature of AD, alternatively, the multi-target-directed ligands (MTDLs) strategy is considered as an effective way.[15,16] It is well-known that many multifunctional agents have been synthesized as therapeutics that possess simultaneously with two or more AD-relevant targets, and the results obtained have been encouraging and convince researchers that MTDLs might present the best pharmacological option for tackling the multifactorial nature of AD and for halting the progression of the disease.[17-19] Further studies suggested the combination of MAO and ChE inhibition in the same molecule as a promising strategy in the treatment of AD.[20]

In the development of IMAOs for the treatment of neurodegenerative diseases, compound **JMC49** was a noticeable MAO-B inhibitor, the 3,4-dihydro-2(1*H*)-quinoline scaffold was catalytic site MAO-B, and spacer was the entrance cavity MAO-B.[21,22] Moreover, the *O*-alkylamine side chains might increase the MAO-A inhibitory activity.[14] Donepezil is approved by the FDA as a selective AChE inhibitor for the treatment of AD. It has been proved that the 1-benzylpiperidine fragment of donepezil is the pharmacophore. Recently, our group has reported the synthesis of genistein-*O*-alkylbenzylamines and scutellarein-*O*-alkylamines as potential multifunctional agents for the treatment of AD, which has showed that the tertiary amino group linked lipophilic moiety binds to the catalytic and mid-gorge sites of AChE.[23,24] Taking the above mentioned into account, based on MTDLs drug design strategy, we plan to fuse the 3,4-dihydro-2(1*H*)-quinoline and tertiary amino with methylene spacers of different lengths, to test whether these novel molecules might possess more potency.

In this work, a series of 3,4-dihydro-2(1*H*)-quinoline-*O*-alkylamine derivatives were designed based on MTDLs (**Figure 1**). They were also synthesized and

evaluated for their multifunctional biological activities, including inhibition of ChE (AChE and BuChE) and MAO (MAO-A and MAO-B), the kinetics of enzyme inhibition, and the ability of cross blood–brain barrier *in vitro,*. Finally, molecular modeling studies were also performed to afford insight into the binding mode and the structure-activity relationships of the novel 3,4-dihydro-2(1*H*)-quinoline-*O*-alkylamine derivatives.

<Insert **Figure 1**>

2. Results and discussion

2.1. Chemistry

The synthetic of 3,4-dihydro-2(1*H*)-quinoline-*O*-alkylamine derivatives were depicted via the general pathway in **Scheme 1**, in which 7-hydroxy-3,4-dihydro-2(1*H*)-quinoline (**1**) was used as the starting material. Alkyation of **1** with excessive amounts of 1,3-dibromopropane (**2a**), 1,4-dibromobutane (**2b**), 1,5 –dibromopentane (**2c**) or 1,6-dibromohexane (**2d**) in the presence of K_2CO_3 in CH_3CN at 60–65°C resulted in the intermediates **3a-d**. In sequence,these intermediates were reacted with the corresponding secondary amines **4a-k** in the presence of K_2CO_3 in CH_3CN at 60–65°C to obtain the final3,4-dihydro-2(1*H*)-quinoline-*O*-alkylamine derivatives **TM1~33**. All new compounds were purified by chromatography, and the analytical and spectroscopic data confirmed their structures, as detailed in the experimental section.

<Insert **Scheme 1**>

2.2. Pharmacology

2.2.1. Inhibition studies on AChE and BuChE

To study the multipotent profile of the 3,4-dihydro-2(1*H*)-quinoline-*O*-alkylamine derivatives, they were first evaluated as inhibitors of AChE and BuChE. The inhibitory activities of target compounds **TM-1~TM-33** against *ee*AChE (from *electric eel*) and *eq*BuChE (from *equine serum*) were measured according to the Ellman assay.[23] Donepezil, a well-known cholinesterase inhibitor, was used as reference standards, the precursor compound

7-hydroxy-3,4-dihydro-2(1*H*)-quinoline (**1**) was also evaluated for comparative purpose. Furthermore, all the compounds were reevaluated using *rat*AChE and *rat* BuChE. The results are listed in **Table 1**, expressed as IC_{50} values. Compared with 7-hydroxy-3,4-dihydro-2(1*H*)-quinoline (**1**) and donepezil, the tested target compounds showed moderate to good potent regarding the inhibition of *Ee*AChE with IC_{50} values ranging from 0.56 to 23.5 μM (**Table 1**). Moreover, they exhibited similar potencies against eqBuChE, as IC_{50} values range from 0.87 to 39.6 μM. Most target compounds displayed slightly selective AChE inhibitors (the ratio IC_{50}(eqBuChE)/IC_{50}(*Ee*AChE) varies from 1.3 to 14.9), except compounds **TM-7**, **TM-12**, **TM-14**, **TM-15**, **TM-19**, **TM-21**, **TM-22**, **TM-23**, **TM-26**, **TM-28**, **TM-29**, **TM-30** and **TM-32**. Accordingly, the length of the linker and the terminal groups NR_1R_2 seem to be a significant factor for the inhibitory potency against AChE and BuChE. The most potent compound was compound **TM-33**, which are characterized by IC_{50} values of 0.56 μM against AChE and IC_{50} values of 2.3 μM against BuChE.

For *Ee*AChE inhibition, the structure-activity relationship is from **Table 1**, although the precursor compound 7-hydroxy-3,4-dihydro-2(1*H*)-quinoline (**1**) did not show significant inhibitory activity, introduction of the *O*-alkylamines observably increased the AChE inhibitory capacity. The results revealed that the terminal groups NR_1R_2 of side chain caused significant effects on AChE inhibitory activities. To be more specific, to start with, compounds **TM-1 ~ TM-30** were synthesized, the data showed that the piperazine substituent (**4e, 4d, 4f**) showed better inhibitory activity than the others (**4a, 4b, 4e, 4g, 4h**). The methylene chain length also was an important factor, with the same terminal groups NR_1R_2, AChE inhibitory activity increased with an increase in methylene chain length, except compounds **TM-9** and **TM-21**, where the optimal chain length was four and five, respectively. However, inhibitory activity decreased with an increase of methylene chain length when the terminal groups NR_1R_2 was 1-(2-pyridyl)piperazine and *N*-benzylpiperazine, for example compounds (**TM-4**, **TM-12, TM-19, TM-26**) and compounds (**TM-6, TM-13, TM-20, TM-28**). It might be that the methylene chain length significantly affect the conformation, further enhance the affinity for AChE *via* intermolecular hydrogen bond, π-π, σ-π

interaction with important amine acid residues, such as **TM-3**-*Tc*AChE complex (**Figure S1A**), **TM-11**-*Tc*AChE (**Figure S1B**), **TM-18**-*Tc*AChE complex (**Figure S1C**) and **TM-25**-*Tc*AChE (**Figure S1D**). Among of these derivatives, compound **TM-25**, with isopropylpyrazine group and six methylene chain, exhibited the best AChE inhibitory activity (IC_{50} = 0.76 μM). In addition, compounds **TM-31~TM-33** was synthesized and evaluated, revealed good inhibitory activity. Among of which, compound **TM-33**, with 4-benzylpiperidine, indicated the higher AChE inhibitory activity (IC_{50} = 0.56 μM) than that of **TM-25**. Furthermore, the optimal compound **TM-33** was re-evaluated using *hu*AChE, and showed a good inhibitory activity with IC_{50} value was 1.02 ± 0.01 μM .

For *eq*BuChE inhibition, generally, the compounds with NR_1R_2 substituent groups **4c, 4g, 4i, 4j** and **4k** displayed better inhibitory potency than that with others. In the same conditions, BuChE inhibitory activity increased with an increase in methylene chain length, except compounds **TM-10** and **TM-21**, where the optimal chain length was four and five, respectively. Compound **TM-32**, with pyrrole, appeared the best BuChE inhibitory activity (IC_{50} = 0.87 μM). Compound **TM-33** also indicated good BuChE inhibitory with IC_{50} value of 2.3 μM. From the re-evaluated results by additional testing using *rat*AChE and *rat*BuChE, it is notable that most of the tested compounds were selective AChE inhibitors and exhibited weaker inhibitory activity towards ChE (*rat*AChE and ratBuChE) than towards ChE (*Ee*AChE and *eq*BuChE), expect compounds **TM-3, TM-7, TM-10, TM-14, TM-17, TM-18, TM-24, TM-25** and **TM-31**, which were selective BuChE inhibitors. Compound **TM-33** presented the highest inhibitory activity toward *rat*AChE and *rat*BuChE with IC_{50} value of 1.9 μM and 3.6 μM, respectively.

<Insert **Table 1**>

2.2.2. Kinetic studies of AChE inhibition

To investigate the AChE inhibitory mechanism for this class of 3,4-dihydro-2(1*H*)-quinoline-*O*-alkylamine derivatives, a kinetic study was carried out with a representative compound **TM-33** using *Ee*AChE (**Figure 2**).[25] The Lineweaver–Burk plots exhibited that both inhibitions had rising slopes and

increasing intercepts at higher concentration, which indicated a mixed-type inhibition. The result demonstrated that compound **TM-33** could bind to both CAS and PAS of AChE.

<Insert **Figure 2**>

2.2.3. Molecular modeling studies

In order to explore possible binding mechanism to AChE and BuChE, a further computational study was performed for compound **TM-33** using the docking program, AutoDock 4.2 package with Discovery Studio 2.5, based on the X-ray crystal structure of *Tc*AChE (PDB code: 1EVE) and *hu*BuChE (PDB code: 4TPK).[23,25] As shown in **Figure 3**, the results indicated that **TM-33** occupied the entire enzymatic CAS, the mid-gorge sites and the PAS, and could simultaneously bind to both the catalytic site and the peripheral site thus providing an explanation for its highly potent inhibitory activity against AChE. In the **TM-33**-*Tc*AChE complex, the 4-benzylpiperidine of moiety of **TM-33** was observed to bind to the CAS *via* a sigma-Pi interaction with TRY334. The long chain of methylene could fold into a conformation in the gorge that allowed them to interact with PHE330 and TYR121 through hydrophobic interaction. In addition, the carbonyl group and NH at the 3,4-dihydro-2(1*H*)-quinoline nucleus could simultaneously bind to the SER124 and TRP84 via two intermolecular hydrogen bonds. The results of the docking in **Figure 4** also showed that compound **TM-33** bind with BuChE via multiple sites. The carbonyl group and NH at the 3,4-dihydro-2(1*H*)-quinoline nucleus could simultaneously bind to the TYR128 via two intermolecular hydrogen bonds. The benzene ring of 3,4-dihydro-2(1*H*)-quinoline nucleus via two Pi-Pi interaction with TRP82. Moreover, hydrophobic interactions could be observed between the ligand and GLY116, GLY117, ALA328, PHE329 and HIS438. Based on these results above, the strong affinity of compound **TM-33** bind to amino acid residues may be partially explained the high potent in inhibiting AChE and BuChE.

<Insert **Figure 3**>

<Insert **Figure 4**>

2.2.4. Recombinant human MAO-A and-B inhibition studies

The synthesized derivatives were tested *in vitro* for their MAO-A and –B inhibitory activities using clorgyline, rasagiline and iproniazid as reference drugs. Recombinant human MAO-A and –B were employed as enzyme sources, and their activities were determined by a fluorimetric method with kynuramine as a common substrate.[14] As shown in **Table 2**, the synthesized target compounds were significantly selective hMAO-A inhibitors, except compounds **TM-1, TM-8, TM-9, TM-10, TM-11, TM-17, TM-22** and **TM-28** were selective hMAO-B inhibitors. All the derivatives displayed moderate to good MAO-A inhibition (IC_{50} values range from 0.3 to 14.3 μM) and significant MAO-B inhibition (IC_{50} values range from 1.4 to 31.7 μM). Among of which, compound **TM-33**, with 4-benzylpiperidine, exhibited the most potent compound toward both isoforms (IC_{50} of 0.3 ± 0.001 μM and 1.4 ± 0.01 μM for MAO-A and MAO-B, respectively). The data appeared that MAO-A inhibitory activity increased with an increase in methylene chain length, except compounds **TM-20**, where the optimal chain length was five. However, inhibitory activity decreased with an increase of methylene chain length when substituent group NR_1R_2 was 1-(2-pyridyl)piperazine, for example compounds (**TM-4**, **TM-12, TM-19, TM-26**). The *O*-alkylamines side chain also had significant effects on MAO-B inhibition. Generally, with the same terminal groups NR_1R_2, MAO-B inhibitory activity increased with an increase in methylene chain length, except compounds **TM-10, TM-11** and **TM-21**, where the optimal chain length was four. However, inhibitory activity decreased with an increase of methylene chain length when the terminal groups NR_1R_2 was piperidine, for example compounds (**TM-1**, **TM-9, TM-16, TM-23**). The terminal groups NR_1R_2 (**4f, 4g, 4h, 4i, 4j** and **4k**) showed good inhibitory potency toward MAO-B inhibition. In particular, compound **TM-33**, with 4-benzylpiperidine, indicated the highest inhibitory activity with IC_{50} values of 1.4 μM.

<Insert **Table 2**>

2.2.5. Cytotoxic effects

To examine the cytotoxicity of the representative compound **TM-33**, PC12 cells were

exposed to the test compound with increasing concentrations (1, 10 and 100 μM) for 24 h, and the cell viability was tested by the 3-(4,5-dimethylthiazol-2-yl)-2,5-diphenyltetrazolium (MTT) assays. As shown in **Figure 5**, **TM-33** did not show modified cell viability up to the concentration of 10 μM. With increased concentration to 100 μM, **TM-33** induced a decrease of cell viability (87.3%). The result showed that the target compound **TM-33** had a wide therapeutic safety range on PC12 cells.

<Insert **Figure 5**>

2.2.6. *In vitro* blood–brain barrier permeation assay

Brain penetration and acute toxicity are major requirements for successful CNS drugs. To evaluate the brain penetration of the compound **TM-33**, we used a parallel artificial membrane assay for the blood- brain barrier (PAMPA-BBB), as described by Di et al.[27,28] We compared the permeability of 11 commercial drugs with reported values to validate the assay (**Table S1**). A plot of the experimental data versus the reported values produced a good linear correlation, P_e (exp) = 0.9163P_e (bibl.) −0.2247 (r^2 = 0.9558) (**Figure S1**). From this equation, and considering the limit established by Di *et al.* for blood–brain barrier permeation, we determined that compounds with permeabilities above 3.44×10^{-6} cm/s could cross the blood–brain barrier (**Table S2**). According to the measured permeability (**Table 3**), as expected, **TM-33** could cross the BBB and reach the biological targets located in the CNS.

<Insert **Table 3**>

2.2.7. Theoretical evaluation of ADME properties.

To correlate better the druglike properties of ferulic acid-donepezil hybrids, the lipophilicity, expressed as the octanol/water partition coefficient and herein called log *P*, as well as other theoretical calculations such as the topological polar surface area (TPSA), the number of hydrogen-bond acceptors, and the number of hydrogen-bond donors were calculated using the Molinspiration property program.[23] The theoretical prediction of the absorption, distribution, metabolism, and excretion (ADME) properties of compound **TM-33** is summarized in **Table 4**.

<Insert **Table 4**>

From the data obtained for the theoretical evaluation of the ADME properties, compound **TM-33** do not break any point of the Lipinski's rule of five, making them promising leads for drug candidates. TPSA and log P values are compatible with those described as a predictive indicator of a drug's capacity for membrane penetration.

3. Conclusion

In conclusion, this article involved the synthesis of a new series of 3,4-dihydro-2(1*H*)-quinoline-*O*-alkylamine derivatives acted as multi-target-directed ligands for the treatment of Alzheimer's disease. Among the synthesized compounds, compound **TM-33** demonstrated the highest AChE and BuChE inhibitory activities with IC_{50} values of 0.56 μM and 2.3 μM, and exhibited favourable hMAO-A (IC_{50} = 0.3 ± 0.001 μM) and hMAO-B (IC_{50} = 1.4 ± 0.01 μM) inhibitory potency. The molecular modeling might play a key role in the structure-activity relationship. The kinetic analysis suggested that **TM-33** showed mixed-type inhibition, and could bind to both CAS and PAS of AChE, which was consistent with the molecular modeling study. More interestingly, our study proved that **TM-33** could cross the blood-brain barrier (BBB) *in vitro*, and complied with Lipinski's rule of five. The present study indicated that **TM-33** could be considered as an interesting multi-targeted lead compound for the further study in the treatment of advanced AD. Further investigations to evaluate compound **TM-33** *in vivo* and to develop structural refinements are in progress and will be reported in due course.

4. Experimental section

4.1. Chemistry

Unless otherwise noted, all materials were obtained from commercial suppliers and used without further purification. The purity of all final compounds was determined by high-performance liquid chromatography (HPLC) analysis to be over 97%. HPLC analysis was carried out on a Waters600-2487 plus system with the use of a Kromasil C_{18} column (4.6 mm × 250 mm, 5um). ^{1}H and ^{13}C NMR spectra were recorded using TMS as the internal standard in $CDCl_3$ with a Varian INOVA spectrometer at 400 and 100 MHz, respectively. Coupling constants were given in Hz.

Multiplicities are given as s (singlet), d (doublet), dd (double-doublet), t (triplet), q (quadruplet), m (multiplet), and br (broad signal). MS spectra data were obtained on an Agilent-6210 TOF LC-MS spectrometer. All the reactions were monitored by thin-layer chromatography (TLC) using silica gel GF_{254} plates from Qingdao Haiyang Chemical Co. Ltd. (China) with an UV lamp (254nm). Column chromatography using silica gel (230–400 mesh) purchased from Qingdao Haiyang Chemical Co. Ltd. (China).

4.1.1. General procedure for the synthesis of intermediates 3a-3d. The appropriate dibromoalkane derivative **2a-2d** (4.4 mmol) was added to a mixture of the starting material 7-hydroxy-3,4-dihydro-2(1*H*)-quinoline (**1**) (2.0 mmol), anhydrous K_2CO_3 (290 mg, 2.1 mmol) in CH_3CN (8 mL)**.** The reaction mixture was heated to 60-65 °C and stirred for 8-10 h under an argon atmosphere. After complete reaction, the solvent was evaporated under reduced pressure. Water (30 mL) was added to the residue and the mixture was extracted with dichloromethane (30 mL × 3). The combined organic phases were washed with saturated aqueous sodium chloride, dried over sodium sulfate, and filtered. The solvent was evaporated to dryness under reduced pressure. The residue was purified on a silica gel chromatography using dichloromethane/acetone (50:1) as eluent to give the intermediates **3a-3d**.

7-(3-Bromopropoxy)-3,4-dihydroquinolin-2(1*H*)-one (3a). Colorless oil, 65.3% yield. ^{1}H NMR (400 MHz, $CDCl_3$) δ 8.15 (s, 1H, CONH), 7.06 (d, *J* = 8.0 Hz, 1H, Ar-H), 6.54 (d, *J* = 8.0 Hz, 1H, Ar-H), 6.35 (s, 1H, Ar-H), 4.08 (t, *J* = 5.6 Hz, 2H, OCH_2), 3.60 (t, *J* = 6.0 Hz, 2H, $BrCH_2$), 2.90 (t, *J* = 7.2 Hz, 2H, $phCH_2$), 2.62 (t, *J* = 7.2 Hz, $COCH_2$), 2.33-2.27 (m, 2H, CH_2).

7-(4-Bromobutoxy)-3,4-dihydroquinolin-2(1*H*)-one (3b). Colorless oil, 68.7% yield. ^{1}H NMR (400 MHz, $CDCl_3$) δ 8.55 (s, 1H, CONH), 7.04 (d, *J* = 8.0 Hz, 1H, Ar-H), 6.51 (d, *J* = 8.0 Hz, 1H, Ar-H), 6.36 (s, 1H, Ar-H), 3.97 (t, *J* = 5.6 Hz, 2H, OCH_2), 3.49 (t, *J* = 6.4 Hz, 2H, $BrCH_2$), 2.89 (t, *J* = 7.2 Hz, 2H, $phCH_2$), 2.62 (t, *J* = 7.2 Hz, $COCH_2$), 2.09-2.02 (m, 2H, CH_2), 1.96-1.89 (m, 2H, CH_2).

7-((5-Bromopentyl)oxy)-3,4-dihydroquinolin-2(1*H*)-one (3c). Colorless oil, 60.2% yield. ^{1}H NMR (400 MHz, $CDCl_3$) δ 8.74 (s, 1H, CONH), 7.06 (d, *J* = 8.0 Hz, 1H,

Ar-H), 6.53 (dd, J_1 = 6.4 Hz, J_2 = 2.0 Hz, 1H, Ar-H), 6.39 (d, J = 2.0 Hz, 1H, Ar-H), 3.96 (t, J = 6.4 Hz, 2H, OCH_2), 3.46 (t, J = 6.4 Hz, 2H, $BrCH_2$), 2.91 (t, J = 7.2 Hz, 2H, $phCH_2$), 2.64 (t, J = 7.2 Hz, $COCH_2$), 1.99-1.91 (m, 2H, CH_2), 1.85-1.77 (m, 2H, CH_2), 1.65-1.61 (m, 2H, CH_2).

7-((6-Bromohexyl)oxy)-3,4-dihydroquinolin-2(1*H*)-one (3d). Colorless oil, 56.8% yield. ^{1}H NMR (400 MHz, $CDCl_3$) δ 9.37 (s, 1H, CONH), 7.04 (d, J = 8.0 Hz, 1H, Ar-H), 6.52 (dd, J_1 = 6.0 Hz, J_2 = 2.0 Hz, 1H, Ar-H), 6.43 (d, J = 1.6 Hz, 1H, Ar-H), 3.94 (t, J = 6.4 Hz, 2H, OCH_2), 3.43 (t, J = 6.8 Hz, 2H, $BrCH_2$), 2.90 (t, J = 7.6 Hz, 2H, $phCH_2$), 2.63 (t, J = 8.0 Hz, $COCH_2$), 1.92-1.87 (m, 2H, CH_2), 1.80-1.76 (m, 2H, CH_2), 1.52-1.49 (m, 4H, 2 × CH_2).

4.1.2. General procedure for the synthesis of 3,4-dihydro-2(1*H*)-quinoline-*O*-alkylamine derivatives TM1~TM31. To a mixture of the corresponding secondary amines **4a~4k** (0.6 mmol), anhydrous K_2CO_3 (89.7 mg, 0.65 mmol) in anhydrous CH_3CN (7 mL) were added the appropriate intermediates **10–13** (0.5 mmol). The reaction mixture was warmed to 60-65 °C and stirred for 6–10 h under an argon atmosphere. After complete reaction, the solvent was evaporated under reduced pressure. The residue was dissolved in water (30 mL) and the mixture was extracted with dichloromethane (20 mL × 3). The combined organic phases were washed with saturated aqueous sodium chloride (30 mL), dried over sodium sulfate, and filtered. The solvent was evaporated to dryness under reduced pressure. The residue was purified on a silica gel chromatography using mixtures of dichloromethane/acetone (30:1) as eluent to afford the corresponding 3,4-dihydro-2(1*H*)-quinoline-*O*-alkylamine derivatives **TM1~TM31.**

7-(3-(Piperidin-1-yl)propoxy)-3,4-dihydroquinolin-2(1*H*)-one (TM-1). Colorless oil, 75.2% yield. 98.2% HPLC purity. ^{1}H NMR (400 MHz, $CDCl_3$) δ 8.45 (s, 1H), 7.03 (d, J = 8.4 Hz, 1H), 6.52 (dd, J_1 = 6.4 Hz, J_2 = 1.6 Hz, 1H), 6.36 (s, 1H), 3.98 (t, J = 6.4 Hz, 2H), 2.89 (t, J = 7.6 Hz, 2H), 2.62 (t, J = 7.6 Hz, 2H), 2.51 (t, J = 7.6 Hz, 2H), 2.46-2.41 (m, 4H), 1.64-1.59 (m, 4H), 1.48-1.42 (m, 2H). MS (ESI) m/z: 289.2 $[M + H]^+$.

7-(3-(Diethylamino)propoxy)-3,4-dihydroquinolin-2(1*H*)-one (TM-2). Colorless

oil, 80.6% yield. 98.6% HPLC purity. ^{1}H NMR (400 MHz, $CDCl_3$) δ 9.23 (s, 1H), 6.95 (d, J = 8.4 Hz, 1H), 6.44 (dd, J_1 = 6.0 Hz, J_2 = 2.4Hz, 1H), 6.36 (d, J = 2.4 Hz, 1H), 3.90 (t, J = 6.0 Hz, 2H), 2.81 (t, J = 7.2 Hz, 2H), 2.60 (t, J = 7.2 Hz, 2H), 2.57-2.51 (m, 4H), 1.91-1.84 (m, 2H), 1.00 (t, J = 7.2 Hz, 6H). MS (ESI) m/z: 277.2 $[M + H]^+$.

7-(3-(4-Isopropylpiperazin-1-yl)propoxy)-3,4-dihydroquinolin-2(1*H*)-one (TM-3). Light yellow oil, 69.4% yield. 98.0% HPLC purity. ^{1}H NMR (400 MHz, $CDCl_3$) δ 8.48 (s, 1H), 7.03 (d, J = 8.4 Hz, 1H), 6.52 (dd, J_1 = 6.0 Hz, J_2 = 2.4 Hz, 1H), 6.35 (d, J = 2.0 Hz, 1H), 3.97 (t, J = 6.4 Hz, 2H), 2.89 (t, J = 7.6 Hz, 2H), 2.71-2.65 (q, J = 6.4 Hz, 1H), 2.61 (t, J = 8.0 Hz, 2H), 2.58-2.50 (m, 10H), 1.99-1.92 (m, 2H), 1.06 (d, J = 6.4 Hz, 6H). MS (ESI) m/z: 332.2 $[M + H]^+$.

7-(3-(4-(Pyridin-2-yl)piperazin-1-yl)propoxy)-3,4-dihydroquinolin-2(1*H*)-one (TM-4). Light yellow oil, 76.8% yield. 98.5% HPLC purity. ^{1}H NMR (400 MHz, $CDCl_3$) δ 8.49 (s, 1H), 8.19 (d, J = 3.6 Hz, 1H), 7.48 (t, J = 7.2 Hz, 1H), 7.04 (d, J = 8.0 Hz, 1H), 6.67-6.61 (m, 2H), 6.53 (dd, J_1 = 6.0 Hz, J_2 = 2.4 Hz, 1H), 6.37 (d, J = 2.0 Hz, 1H), 4.02 (t, J = 6.0 Hz, 2H), 3.59 (t, J = 8.4 Hz, 4H), 2.89 (t, J = 7.2 Hz, 2H), 2.63-2.59 (m, 8H), 2.06-1.99 (m, 2H). MS (ESI) m/z: 367.2 $[M + H]^+$.

7-(3-(4-(Pyrrolidin-1-yl)piperidin-1-yl)propoxy)-3,4-dihydroquinolin-2(1*H*)-one (TM-5). Light yellow oil, 84.1% yield. 98.0% HPLC purity. ^{1}H NMR (400 MHz, $CDCl_3$) δ 8.98 (s, 1H), 7.02 (d, J = 8.4 Hz, 1H), 6.67-6.61 (m, 2H), 6.51 (dd, J_1 = 6.0 Hz, J_2 = 2.0 Hz, 1H), 6.42 (d, J = 2.0 Hz, 1H), 3.98 (t, J = 6.0 Hz, 2H), 2.98 (d, J = 11.2 Hz, 2H), 2.88 (t, J = 8.0 Hz, 2H), 2.80-2.76 (m, 4H), 2.61 (t, J = 8.0 Hz, 2H), 2.51 (t, J = 7.2 Hz, 2H), 2.30 (t, J = 6.8 Hz, 1H), 2.03 (t, J = 10.8 Hz, 2H), 1.98-1.86 (m, 8H), 1.76-1.68 (m, 2H). MS (ESI) m/z: 358.2 $[M + H]^+$.

7-(3-(4-Benzylpiperazin-1-yl)propoxy)-3,4-dihydroquinolin-2(1*H*)-one (TM-6). Light yellow oil, 63.9% yield. 97.8% HPLC purity. ^{1}H NMR (400 MHz, $CDCl_3$) δ 9.39 (s, 1H), 7.33-7.24 (m, 5H), 7.03 (d, J = 8.4 Hz, 1H), 6.52 (dd, J_1 = 5.6 Hz, J_2 = 2.4 Hz, 1H), 6.41 (d, J = 2.4 Hz, 1H), 3.97 (t, J = 6.0 Hz, 2H), 3.53 (s, 2H), 2.89 (t, J = 8.0 Hz, 2H), 2.62 (t, J = 8.0 Hz, 2H), 2.58-2.46 (m, 10H), 1.99-1.92 (m, 2H). MS (ESI) m/z: 380.2 $[M + H]^+$.

7-(3-(3,4-Dihydroisoquinolin-2(1H)-yl)propoxy)-3,4-dihydroquinolin-2(1*H*)-one (TM-7). Colorless oil, 67.6% yield. 98.9% HPLC purity. ^{1}H NMR (400 MHz, $CDCl_3$) δ 9.40 (s, 1H), 7.12-6.98 (m, 5H), 6.52 (dd, J_1 = 6.0 Hz, J_2 = 2.4 Hz, 1H), 6.41 (d, J = 2.0 Hz, 1H), 4.00 (t, J = 6.0 Hz, 2H), 3.65 (s, 2H), 2.90 (t, J = 5.6 Hz, 2H), 2.85 (t, J = 8.0 Hz, 2H), 2.75 (t, J = 5.6 Hz, 2H), 2.68 (t, J = 7.2 Hz, 2H), 2.59 (t, J = 7.6 Hz, 2H), 2.08-2.02 (m, 2H). ^{13}C NMR (100 MHz, $CDCl_3$) 172.53, 158.69, 138.35, 134.74, 134.32, 128.69, 128.53, 126.61, 126.18, 125.66, 115.69, 108.80, 102.43, 66.43, 56.20, 54.93, 51.03, 31.10, 29.11, 27.06, 24.58. MS (ESI) m/z: 337.2 $[M + H]^+$.

7-(3-(Benzyl(prop-2-yn-1-yl)amino)propoxy)-3,4-dihydroquinolin-2(1*H*)-one (TM-8). Colorless oil, 66.7% yield. 98.5% HPLC purity. ^{1}H NMR (400 MHz, $CDCl_3$) δ 7.68 (s, 1H), 7.36-7.27 (m, 5H), 7.06 (d, J = 8.4 Hz, 1H), 6.54 (dd, J_1 = 6.4 Hz, J_2 = 1.6 Hz, 1H), 6.29 (d, J = 1.6 Hz, 1H), 4.02 (t, J = 6.4 Hz, 2H), 3.68 (s, 2H), 3.36 (d, J = 1.6 Hz, 2H), 2.92 (t, J = 7.2 Hz, 2H), 2.75 (t, J = 6.8 Hz, 2H), 2.64 (t, J = 7.2 Hz, 2H), 2.25 (s, 1H), 2.01-1.94 (m, 2H). MS (ESI) m/z: 349.2 $[M + H]^+$.

7-(4-(Piperidin-1-yl)butoxy)-3,4-dihydroquinolin-2(1*H*)-one (TM-9). Light yellow oil, 68.7% yield. 98.1% HPLC purity. ^{1}H NMR (400 MHz, $CDCl_3$) δ 9.19 (s, 1H), 7.02 (d, J = 8.4 Hz, 1H), 6.51 (d, J = 7.6 Hz, 1H), 6.40 (s, 1H), 3.94 (t, J = 6.0 Hz, 2H), 2.89 (t, J = 7.2 Hz, 2H), 2.62 (t, J = 7.6 Hz, 2H), 2.43-2.33 (m, 6H), 1.79-1.72 (m, 2H), 1.69-1.64 (m, 2H), 1.60-1.57 (m, 4H), 1.46-1.42 (m, 2H, CH_2). MS (ESI) m/z: 312.2 $[M + H]^+$.

7-(4-(Diethylamino)butoxy)-3,4-dihydroquinolin-2(1*H*)-one (TM-10). Colorless oil, 83.5% yield. 98.6% HPLC purity. ^{1}H NMR (400 MHz, $CDCl_3$) δ 8.55 (s, 1H), 6.96 (d, J = 8.4 Hz, 1H), 6.44 (dd, J_1 = 6.0 Hz, J_2 = 2.4 Hz, 1H), 6.32 (d, J = 2.4 Hz, 1H), 3.89 (t, J = 5.6 Hz, 2H), 2.82 (t, J = 8.0 Hz, 2H), 2.71 (q, J = 7.2 Hz, 4H), 2.65 (t, J = 7.6 Hz, 2H), 2.54 (t, J = 8.0 Hz, 2H), 1.75-1.68 (m, 4H), 1.10 (t, J = 7.6 Hz, 2H). ^{13}C NMR (100 MHz, $CDCl_3$) 172.00, 158.07, 138.56, 128.43, 115.89, 108.74, 102.50, 67.07, 51.05, 46.64, 31.01, 26.32, 24.48, 20.47, 8.68. MS (ESI) m/z: 291.2 $[M + H]^+$.

7-(4-(4-Isopropylpiperazin-1-yl)butoxy)-3,4-dihydroquinolin-2(1*H*)-one (TM-11). Light yellow oil, 67.1% yield. 98.2% HPLC purity. ^{1}H NMR (400 MHz, $CDCl_3$) δ 7.95 (s, 1H), 7.04 (d, J = 8.4 Hz, 1H), 6.51 (dd, J_1 = 6.0 Hz, J_2 = 2.4 Hz, 1H), 6.30 (d,

J = 2.4 Hz, 1H), 3.94 (t, *J* = 6.4 Hz, 2H), 2.90 (t, *J* = 7.6 Hz, 2H), 2.74-2.52 (m, 11H), 2.42 (t, *J* = 7.6 Hz, 2H), 1.82-1.75 (m, 2H), 1.71-1.63 (m, 2H), 1.09 (d, J = 6.4 Hz, 6H). ^{13}C NMR (100 MHz, $CDCl_3$) 172.14, 158.41, 138.46, 128.41, 115.64, 108.76, 102.38, 67.54, 57.12, 56.27, 50.61, 47.40, 31.04, 26.84, 24.50, 22.62, 17.36. MS (ESI) m/z: 346.2 $[M + H]^+$.

7-(4-(4-(Pyridin-2-yl)piperazin-1-yl)butoxy)-3,4-dihydroquinolin-2(1*H*)-one (TM-12). Light yellow oil, 60.8% yield. 98.0% HPLC purity. ^{1}H NMR (400 MHz, $CDCl_3$) δ 9.07 (s, 1H), 8.19 (d, *J* = 2.4 Hz, 1H), 7.50-7.45 (m, 1H), 7.03 (t, *J* = 8.0 Hz, 1H), 6.66-6.60 (m, 2H), 6.52 (dd, J_1 = 5.6 Hz, J_2 = 2.4 Hz, 1H), 6.37 (d, *J* = 13.6 Hz, 1H), 3.96 (t, *J* = 5.6 Hz, 2H), 3.57-3.53 (m, 4H), 2.91-2.86 (m, 2H), 2.64-2.57 (m, 6H), 2.48-2.43 (m, 2H), 1.85-1.78 (m, 2H), 1.75-1.71 (m, 2H). MS (ESI) m/z: 381.2 $[M + H]^+$.

7-(4-(4-Benzylpiperazin-1-yl)butoxy)-3,4-dihydroquinolin-2(1*H*)-one (TM-13). Light yellow oil, 68.7% yield. 97.8% HPLC purity. ^{1}H NMR (400 MHz, $CDCl_3$) δ 8.28 (s, 1H), 7.34-7.25 (m, 5H), 7.05 (d, *J* = 8.4 Hz, 1H), 6.52 (dd, J_1 = 6.0 Hz, J_2 = 2.0 Hz, 1H), 6.34 (d, *J* = 2.4 Hz, 1H), 3.95 (t, *J* = 6.4 Hz, 2H), 3.53 (s, 2H), 2.91 (t, *J* = 7.6 Hz, 2H), 2.63 (t, *J* = 8.0 Hz, 2H), 2.56-2.46 (m, 8H), 2.42 (t, *J* = 7.6 Hz, 2H), 1.81-1.75 (m, 2H), 1.71-1.64 (m, 2H). MS (ESI) m/z: 394.2 $[M + H]^+$.

7-(4-(3,4-Dihydroisoquinolin-2(1H)-yl)butoxy)-3,4-dihydroquinolin-2(1*H*)-one (TM-14). Light yellow oil, 73.5% yield. 98.3% HPLC purity. ^{1}H NMR (400 MHz, $CDCl_3$) δ 8.52 (s, 1H), 7.15-7.10 (m, 3H), 7.06-7.03 (m, 2H), 6.54 (dd, J_1 = 6.4 Hz, J_2 = 2.0 Hz, 1H), 6.38 (d, *J* = 2.0 Hz, 1H), 3.99 (t, *J* = 6.0 Hz, 2H), 3.67 (s, 2H), 2.95-2.88 (m, 4H), 2.77 (t, *J* = 6.0 Hz, 2H), 2.63 (t, *J* = 7.6 Hz, 2H), 2.60 (t, *J* = 6.0 Hz, 2H), 1.90-1.76 (m, 4H). ^{13}C NMR (100 MHz, $CDCl_3$) 171.97, 158.70, 138.18, 134.75, 134.31, 128.66, 128.62, 126.60, 126.14, 125.61, 115.68, 108.78, 102.26, 67.94, 57.93, 56.14, 50.92, 31.11, 29.07, 27.24, 24.59, 23.68. MS (ESI) m/z: 351.2 $[M + H]^+$.

7-(4-(Benzyl(prop-2-yn-1-yl)amino)butoxy)-3,4-dihydroquinolin-2(1*H*)-one (TM-15). Light yellow oil, 69.3% yield. 97.6% HPLC purity. ^{1}H NMR (400 MHz, $CDCl_3$) δ 8.96 (s, 1H), 7.38-7.27 (m, 5H), 7.05 (d, *J* = 8.0 Hz, 1H), 6.53 (dd, J_1 = 6.8

Hz, J_2 = 1.6 Hz, 1H), 6.40 (d, J = 1.6 Hz, 1H), 3.95 (t, J = 6.4 Hz, 2H), 3.66 (s, 2H), 3.36 (s, 2H), 2.91 (t, J = 7.6 Hz, 2H), 2.64 (t, J = 6.8 Hz, 4H), 2.27 (s, 1H), 1.88-1.81 (m, 2H), 1.74-1.66 (m, 2H). MS (ESI) m/z: 363.2 $[M + H]^+$.

7-((5-(Piperidin-1-yl)pentyl)oxy)-3,4-dihydroquinolin-2(1*H*)-one (TM-16). Colorless oil, 88.9% yield. 99.2% HPLC purity. ^{1}H NMR (400 MHz, $CDCl_3$) δ 8.83 (s, 1H), 7.03 (d, J = 8.4 Hz, 1H), 6.51 (d, J = 8.4 Hz, 1H), 6.38 (s, 1H), 3.92 (t, J = 6.4 Hz, 2H), 2.89 (t, J = 7.6 Hz, 2H), 2.62 (t, J = 7.6 Hz, 2H), 2.48-2.41 (m, 4H), 2.36 (t, J = 7.2 Hz, 2H), 1.81-1.74 (m, 2H), 1.64-1.55 (m, 6H), 1.49-1.41 (m, 4H). MS (ESI) m/z: 317.2 $[M + H]^+$.

7-((5-(Diethylamino)pentyl)oxy)-3,4-dihydroquinolin-2(1*H*)-one (TM-17). Light yellow oil, 87.6% yield. 98.6% HPLC purity. ^{1}H NMR (400 MHz, $CDCl_3$) δ 9.18 (s, 1H), 6.94 (d, J = 8.0 Hz, 1H), 6.43-6.40 (m, 2H), 3.86 (t, J = 6.0 Hz, 2H), 2.85 (q, J = 7.2 Hz, 4H), 2.80 (t, J = 7.6 Hz, 2H), 2.73 (t, J = 8.0 Hz, 2H), 2.52 (t, J = 8.0 Hz, 2H), 1.75-1.64 (m, 4H), 1.18 (t, J = 7.6 Hz, 6H), 1.47-1.39 (m, 2H). ^{13}C NMR (100 MHz, $CDCl_3$) 172.04, 158.35, 138.47, 128.43, 115.68, 108.82, 102.43, 67.51, 51.32, 46.58, 31.05, 28.43, 24.50, 23.49, 23.15, 8.63. MS (ESI) m/z: 305.2 $[M + H]^+$.

7-((5-(4-Isopropylpiperazin-1-yl)pentyl)oxy)-3,4-dihydroquinolin-2(1*H*)-one (TM-18). Light yellow oil, 83.9% yield. 98.4% HPLC purity. ^{1}H NMR (400 MHz, $CDCl_3$) δ 8.45 (s, 1H), 7.03 (d, J = 8.4 Hz, 1H), 6.51 (d, J = 8.0 Hz, 1H), 6.35 (s, 1H), 3.92 (t, J = 6.4 Hz, 2H), 2.89 (t, J = 7.2 Hz, 2H), 2.68-2.45 (m, 11H), 2.37 (t, J = 8.0 Hz, 2H), 1.82-1.74 (m, 2H), 1.61-1.53 (m, 2H), 1.50-1.42 (m, 2H), 1.06 (d, J = 6.4 Hz, 6H). MS (ESI) m/z: 360.3 $[M + H]^+$.

7-((5-(4-(Pyridin-2-yl)piperazin-1-yl)pentyl)oxy)-3,4-dihydroquinolin-2(1*H*)-one (TM-19). Light yellow oil, 82.6% yield. 98.0% HPLC purity. ^{1}H NMR (400 MHz, $CDCl_3$) δ 8.60 (s, 1H), 8.20 (d, J = 7.2 Hz, 1H), 7.49 (t, J = 8.8 Hz, 1H), 7.04 (d, J = 8.4 Hz, 1H), 6.67-6.62 (m, 2H), 6.52 (dd, J_1 = 6.0 Hz, J_2 = 2.4 Hz, 1H), 6.38 (d, J = 2.4 Hz, 1H), 3.94 (t, J = 6.4 Hz, 2H), 3.61-3.56 (m, 4H), 2.90 (t, J = 8.0 Hz, 2H), 2.64-2.58 (m, 6H), 2.45 (t, J = 8.0 Hz, 2H), 1.84-1.77 (m, 2H), 1.69-1.59 (m, 2H), 1.54-1.47 (m, 2H). MS (ESI) m/z: 395.2 $[M + H]^+$.

7-((5-(4-Benzylpiperazin-1-yl)pentyl)oxy)-3,4-dihydroquinolin-2(1*H*)-one

(TM-20). Light yellow oil, 80.7% yield. 98.8% HPLC purity. ^{1}H NMR (400 MHz, $CDCl_3$) δ 8.34 (s, 1H), 7.33 (d, *J* = 8.4 Hz, 4H), 7.28-7.24 (m, 1H), 7.05 (d, *J* = 8.4 Hz, 1H), 6.52 (dd, J_1 = 5.6 Hz, J_2 = 2.4 Hz, 1H), 6.34 (d, *J* = 2.4 Hz, 1H), 3.93 (t, *J* = 6.4 Hz, 2H), 3.53 (s, 2H), 2.91 (t, *J* = 8.0 Hz, 2H), 2.63 (t, *J* = 8.0 Hz, 2H), 2.54-2.42 (m, 8H), 2.38 (t, *J* = 8.0 Hz, 2H), 1.83-1.75 (m, 2H), 1.61-1.54 (m, 2H), 1.51-1.43 (m, 2H). MS (ESI) m/z: 408.3 $[M + H]^+$.

7-((5-(3,4-Dihydroisoquinolin-2(1H)-yl)pentyl)oxy)-3,4-dihydroquinolin-2(1*H*)-one (TM-21). ^{1}H NMR (400 MHz, $CDCl_3$) δ 8.34 (s, 1H), 7.33 (d, *J* = 8.4 Hz, 4H), 7.28-7.24 (m, 1H), 7.05 (d, *J* = 8.4 Hz, 1H), 6.52 (dd, J_1 = 5.6 Hz, J_2 = 2.4 Hz, 1H), 6.34 (d, *J* = 2.4 Hz, 1H), 3.93 (t, *J* = 6.4 Hz, 2H), 3.53 (s, 2H), 2.91 (t, *J* = 8.0 Hz, 2H), 2.63 (t, *J* = 8.0 Hz, 2H), 2.54-2.42 (m, 8H), 2.38 (t, *J* = 8.0 Hz, 2H), 1.83-1.75 (m, 2H), 1.61-1.54 (m, 2H), 1.51-1.43 (m, 2H). ^{13}C NMR (100 MHz, $CDCl_3$) 172.17, 158.74, 138.23, 134.77, 134.31, 128.65, 128.57, 126.60, 126.11, 125.59, 115.62, 108.76, 102.30, 68.02, 58.29, 56.18, 51.00, 31.10, 29.18, 29.04, 26.91, 24.58, 24.08. MS (ESI) m/z: 365.2 $[M + H]^+$.

7-((5-(Benzyl(prop-2-yn-1-yl)amino)pentyl)oxy)-3,4-dihydroquinolin-2(1*H*)-one (TM-22). Light yellow oil, 82.6% yield. 98.2% HPLC purity. ^{1}H NMR (400 MHz, $CDCl_3$) δ 9.08 (s, 1H), 7.38-7.27 (m, 5H), 7.05 (d, *J* = 8.0 Hz, 1H), 6.54 (d, *J* = 8.0 Hz, 1H), 6.41 (s, 1H), 3.94 (t, *J* = 6.4 Hz, 2H), 3.65 (s, 2H), 3.34 (s, 2H), 2.91 (t, *J* = 7.6 Hz, 2H), 2.64 (t, *J* = 7.6 Hz, 2H), 2.60 (t, *J* = 7.2 Hz, 2H), 2.26 (s, 1H), 1.83-1.76 (m, 2H), 1.64-1.56 (m, 2H), 1.55-1.48 (m, 2H). MS (ESI) m/z: 377.2 $[M + H]^+$.

7-((6-(Piperidin-1-yl)hexyl)oxy)-3,4-dihydroquinolin-2(1*H*)-one (TM-23). Colorless oil, 87.5% yield. 98.7% HPLC purity. ^{1}H NMR (400 MHz, $CDCl_3$) δ 8.44 (s, 1H), 7.03 (d, *J* = 8.0 Hz, 1H), 6.51 (d, *J* = 8.4 Hz, 1H), 6.36 (s, 1H), 3.91 (t, *J* = 6.4 Hz, 2H), 2.89 (t, *J* = 8.0 Hz, 2H), 2.61 (t, *J* = 8.0 Hz, 2H), 2.58-2.51 (m, 4H), 2.45 (t, *J* = 8.0 Hz, 2H), 1.78-1.66 (m, 6H), 1.65-1.58 (m, 2H), 1.51-1.44 (m, 4H), 1.40-1.33 (m, 2H). MS (ESI) m/z: 331.2 $[M + H]^+$.

7-((6-(Diethylamino)hexyl)oxy)-3,4-dihydroquinolin-2(1*H*)-one (TM-24). Light yellow oil, 82.9% yield. 98.7% HPLC purity. ^{1}H NMR (400 MHz, $CDCl_3$) δ 9.19 (s, 1H), 6.96 (d, *J* = 8.0 Hz, 1H), 6.44 (dd, J_1 = 6.0 Hz, J_1 = 2.4 Hz, 1H), 6.34 (d, *J* = 2.4

Hz, 1H), 3.84 (t, *J* = 6.4 Hz, 2H), 2.81 (t, *J* = 7.6 Hz, 2H), 2.54 (t, *J* = 8.0 Hz, 2H), 2.47 (q, *J* = 7.2 Hz, 4H), 2.36 (d, *J* = 8.0 Hz, 2H), 1.72-1.64 (m, 2H), 1.45-1.35 (m, 4H), 1.30-1.22 (m, 2H), 0.96 (t, *J* = 7.6 Hz, 6H). MS (ESI) m/z: 319.2 $[M + H]^+$.

7-((6-(4-Isopropylpiperazin-1-yl)hexyl)oxy)-3,4-dihydroquinolin-2(1*H*)-one (TM-25). Light yellow oil, 79.5% yield. 98.1% HPLC purity. ^{1}H NMR (400 MHz, $CDCl_3$) δ 9.59 (s, 1H), 6.93 (d, *J* = 8.0 Hz, 1H), 6.42 (d, *J* = 8.0 Hz, 1H), 6.37 (s, 1H), 3.82 (t, *J* = 6.0 Hz, 2H), 2.79 (t, *J* = 6.4 Hz, 2H), 2.68-2.44 (m, 11H), 2.28 (t, *J* = 5.6 Hz, 2H), 1.72-1.65 (m, 2H), 1.48-1.42 (m, 2H), 1.40-1.35 (m, 2H), 1.32-1.25 (m, 2H), 0.99 (d, *J* = 6.0 Hz, 6H). ^{13}C NMR (100 MHz, $CDCl_3$) 172.42, 158.67, 138.33, 128.41, 115.48, 108.71, 102.30, 67.94, 58.53, 54.58, 53.19, 48.43, 31.05, 29.11, 27.28, 26.63, 25.92, 24.53, 18.47. MS (ESI) m/z: 374.3 $[M + H]^+$.

7-((6-(4-(Pyridin-2-yl)piperazin-1-yl)hexyl)oxy)-3,4-dihydroquinolin-2(1*H*)-one (TM-26). Light yellow oil, 80.2% yield. 98.8% HPLC purity. ^{1}H NMR (400 MHz, $CDCl_3$) δ 8.13 (d, *J* = 4.0 Hz, 1H), 8.02 (s, 1H), 7.44 (t, *J* = 7.6 Hz, 1H), 6.97 (d, *J* = 8.4 Hz, 1H), 6.60 (t, *J* = 8.4 Hz, 2H), 6.44 (d, *J* = 8.0 Hz, 1H), 6.28 (s, 1H), 3.85 (t, *J* = 6.0 Hz, 2H), 3.72-3.69 (m, 4H), 2.84-2.74 (m, 6H), 2.59-2.52 (m, 4H), 1.73-1.66 (m, 4H), 1.45-1.40 (m, 2H), 1.38-1.32 (m, 2H). MS (ESI) m/z: 409.3 $[M + H]^+$.

7-((6-(4-(Pyrrolidin-1-yl)piperidin-1-yl)hexyl)oxy)-3,4-dihydroquinolin-2(1*H*)-one (TM-27). Light yellow oil, 79.5% yield. 98.4% HPLC purity. ^{1}H NMR (400 MHz, $CDCl_3$) δ 8.22 (s, 1H), 7.44 (t, *J* = 7.6 Hz, 1H), 6.97 (d, *J* = 8.4 Hz, 1H), 6.44 (dd, J_1 = 6.0 Hz, J_1 = 2.0 Hz, 1H), 6.27 (s, 1H), 3.84 (t, *J* = 6.4 Hz, 2H), 2.89-2.85 (m, 2H), 2.82 (t, *J* = 7.6 Hz, 2H), 2.57-2.52 (m, 6H), 2.25 (t, *J* = 7.6 Hz, 2H), 2.04-1.98 (m, 1H), 1.90 (t, *J* = 7.6 Hz, 2H), 1.83 (d, *J* = 12.8 Hz, 2H), 1.75-1.65 (m, 6H), 1.59-1.51 (m, 2H), 1.49-1.42 (m, 2H), 1.41-1.35 (m, 2H), 1.32-1.26 (m, 2H). MS (ESI) m/z: 400.3 $[M + H]^+$.

7-((6-(4-Benzylpiperazin-1-yl)hexyl)oxy)-3,4-dihydroquinolin-2(1*H*)-one (TM-28). Light yellow oil, 83.6% yield. 98.0% HPLC purity. ^{1}H NMR (400 MHz, $CDCl_3$) δ 8.62 (s, 1H), 7.34 (d, *J* = 4.4 Hz, 4H), 7.29-7.24 (m, 1H), 7.05 (d, *J* = 8.4 Hz, 1H), 6.53 (dd, J_1 = 6.0 Hz, J_2 = 2.4 Hz, 1H), 6.35 (dd, J_1 = 9.2 Hz, J_2 = 2.0 Hz, 1H), 3.92 (t, *J* = 6.4Hz, 2H), 3.53 (s, 2H), 2.91 (t, *J* = 7.6 Hz, 2H), 2.63 (t, *J* = 8.0 Hz, 2H),

2.59-2.39 (m, 8H), 2.35 (t, *J* = 8.0 Hz, 2H), 1.81-1.74 (m, 2H), 1.57-1.44 (m, 4H), 1.40-1.32 (m, 2H). MS (ESI) m/z: 422.3 $[M + H]^+$.

7-((6-(3,4-Dihydroisoquinolin-2(1H)-yl)hexyl)oxy)-3,4-dihydroquinolin-2(1*H*)-one (TM-29). Light yellow oil, 76.1% yield. 98.1% HPLC purity. ^{1}H NMR (400 MHz, $CDCl_3$) δ 8.96 (s, 1H), 7.12-7.08 (m, 3H), 7.03-7.01 (m, 2H), 6.51 (dd, J_1 = 6.4 Hz, J_2 = 2.0 Hz, 1H), 6.38 (d, *J* = 2.0 Hz, 1H), 3.92 (t, *J* = 6.4 Hz, 2H), 3.64 (s, 2H), 2.92-2.86 (m, 4H), 2.74 (t, *J* = 2.0 Hz, 2H), 2.61 (t, *J* = 8.0 Hz, 2H), 2.52 (t, *J* = 8.0 Hz, 2H), 1.81-1.74 (m, 2H), 1.68-1.60 (m, 2H), 1.54-1.46 (m, 2H), 1.45-1.38 (m, 2H). ^{13}C NMR (100 MHz, $CDCl_3$) 172.16, 158.77, 138.22, 134.74, 134.31, 128.65, 128.57, 126.61, 126.12, 125.60, 115.61, 108.76, 102.29, 68.09, 58.36, 56.17, 50.98, 31.11, 29.20, 29.01, 27.34, 27.09, 26.03, 24.59. MS (ESI) m/z: 379.2 $[M + H]^+$.

7-((6-(Benzyl(prop-2-yn-1-yl)amino)hexyl)oxy)-3,4-dihydroquinolin-2(1*H*)-one (TM-30). Light yellow oil, 76.8% yield. 98.3% HPLC purity. ^{1}H NMR (400 MHz, $CDCl_3$) δ 9.21 (s, 1H), 7.38-7.31 (m, 4H), 7.29-7.25 (m, 1H), 7.05 (d, *J* = 8.4 Hz, 1H), 6.54 (dd, J_1 = 6.0 Hz, J_2 = 2.0 Hz, 1H), 6.44 (d, *J* = 2.0 Hz, 1H), 3.94 (t, *J* = 6.4 Hz, 2H), 3.65 (s, 2H), 3.35 (d, *J* = 1.6 Hz, 2H), 2.91 (t, *J* = 7.6 Hz, 2H), 2.64 (t, *J* = 7.2 Hz, 2H), 2.58 (t, *J* = 7.2 Hz, 2H), 2.26 (s, 1H), 1.82-1.75 (m, 2H), 1.60-1.53 (m, 2H), 1.51-1.40 (m, 4H). MS (ESI) m/z: 391.2 $[M + H]^+$.

7-((5-(Benzyl(ethyl)amino)pentyl)oxy)-3,4-dihydroquinolin-2(1*H*)-one (TM-31). Light yellow oil, 87.2% yield. 98.9% HPLC purity. ^{1}H NMR (400 MHz, $CDCl_3$) δ 9.72 (s, 1H), 7.35 (d, *J* = 7.2 Hz, 2H), 7.29 (t, *J* = 7.2 Hz, 2H), 7.22 (t, *J* = 7.2 Hz, 1H), 6.99 (d, *J* = 8.0 Hz, 1H), 6.47 (t, J = 8.4 Hz, 2H), 3.88 (t, *J* = 6.0 Hz, 2H), 3.59 (s, 2H), 2.85 (t, *J* = 7.2 Hz, 2H), 2.59 (t, *J* = 7.2 Hz, 2H), 2.54 (q, *J* = 7.2 Hz, 2H), 2.47 (t, *J* = 7.2 Hz, 2H), 1.75-1.68 (m, 2H), 1.58-1.51 (m, 2H), 1.46-1.39 (m, 2H), 1.05 (t, *J* = 7.2 Hz, 3H). ^{13}C NMR (100 MHz, $CDCl_3$) 172.68, 158.78, 139.30, 138.39, 129.03, 128.49, 128.22, 126.93, 115.54, 108.86, 102.43, 68.05, 57.99, 52.96, 47.29, 31.10, 29.73, 29.14, 26.61, 24.58, 23.91, 11.58. MS (ESI) m/z: 367.2 $[M + H]^+$.

7-((5-(Pyrrolidin-1-yl)pentyl)oxy)-3,4-dihydroquinolin-2(1*H*)-one (TM-32). Light yellow oil, 88.1% yield. 99.2% HPLC purity. ^{1}H NMR (400 MHz, $CDCl_3$) δ 9.35 (s, 1H), 6.93 (d, *J* = 8.0 Hz, 1H), 6.42-6.39 (m, 2H), 3.84 (t, *J* = 6.0 Hz, 2H), 2.79 (t, *J* =

7.6 Hz, 2H), 2.74-2.68 (m, 4H), 2.59 (t, *J* = 8.0 Hz, 2H), 2.52 (t, *J* = 7.6 Hz, 2H), 1.84-1.79 (m, 4H), 1.72-1.66 (m, 2H), 1.65-1.58 (m, 2H), 1.45-1.38 (m, 2H). ^{13}C NMR (100 MHz, $CDCl_3$) 172.28, 158.59, 138.37, 128.45, 115.58, 108.75, 102.35, 67.81, 56.05, 53.97, 31.07, 29.65, 28.89, 27.56, 24.54, 23.90, 23.34.MS (ESI) m/z: 303.2 $[M + H]^+$.

7-((6-(4-Benzylpiperidin-1-yl)hexyl)oxy)-3,4-dihydroquinolin-2(1*H*)-one (TM-33). Light yellow oil, 89.0% yield. 98.2% HPLC purity. ^{1}H NMR (400 MHz, $CDCl_3$) δ 9.78 (s, 1H), 7.27-7.22 (m, 2H), 7.18-7.09 (m, 3H), 6.99 (t, *J* = 7.6 Hz, 1H), 6.50-6.43 (m, 2H), 3.87 (t, *J* = 6.0 Hz, 2H), 2.96 (d, *J* = 10.0 Hz, 2H), 2.83 (t, *J* = 7.2 Hz, 2H), 2.61-2.55 (m, 2H), 2.52 (t, *J* = 6.0 Hz, 2H), 2.37-2.33 (m, 2H), 1.90 (t, *J* = 11.2 Hz, 2H), 1.79-1.69 (m, 2H), 1.63 (d, *J* = 12.4 Hz, 2H), 1.56-1.50 (m, 3H), 1.46-1.40 (m, 2H), 1.38-1.30 (m, 4H). ^{13}C NMR (100 MHz, $CDCl_3$) 172.56, 158.74, 140.56, 138.41, 129.11, 128.47, 128.18, 125.81, 115.51, 108.80, 102.40, 68.00, 58.87, 53.85, 43.10, 37.82, 31.82, 31.10, 29.71, 29.16, 27.39, 26.63, 25.96, 24.57. MS (ESI) m/z: 421.3 $[M + H]^+$.

4.2. Biological assay.

4.2.1 Inhibition experiments of AChE and BuChE

Acetylcholinesterase (*ee*AChE, from the electric eel; *hu*AChE, from human erythrocytes AChE), butyrylcholinesterase (*eq*BuChE, from equine serum; *hu*BuChE, human serum BuChE), 5,5'-dithiobis-2-nitrobenzoic acid (Ellman's reagent, DTNB), acetylthiocholine chloride (ATC), and butyrylthiocholine chloride (BTC) were purchased form Sigma Aldrich. *rat*AChE and *rat* BuChE was from Institute of Traditional Chinese Medicine Pharmacology and Toxicology, Sichuan Academy of Chinese Medicine Sciences.

The determination of AChE and BuChE inhibitory capacity of the compounds were tested by Ellman assay with slight modification.[23] For AChE inhibition assays, a reaction mixture (100 μL) containing ATC (1 mmol/L, 30 μL), phosphate-buffered solution (0.1 M KH_2PO_4/K_2HPO_4, PH = 8.0, 40 μL), 10 μL enzyme (EeAChE or HuAChE 0.45 U/mL, rat AChE 5% homogenate) and different concentrations (DMSO < 1%) of test compounds (20 μL) was incubated at 37°C for 15 min. Then

5,5'-dithiobis-2-nitrobenzoic acid (DTNB, 0.2%, 30 μL) was added. The activities were determined by using a Varioskan Flash Multimode Reader at 412 nm. Each concentration was assayed in triplicate. The inhibition percent was calculated by the following expression: $(1-A_i/A_c) \times 100$, where A_i and A_c are the absorbance obtained for AChE in the presence and absence of inhibitors, respectively. *In vitro* BuChE assay was performed using a method similar as described above.

4.2.2. Kinetic Characterization of AChE Inhibition

Kinetic characterization of AChE inhibition was performed based on a reported method using purified AChE from *Electrophorus electricus* (*Ee*AChE).[24] The assay solution (100 μL) consists of 0.1 M phosphate buffer (pH 8.0), with the addition of 30 μL of 0.2% DTNB, 10 μL of 0.5 units/mL *Ee*AChE, and 20 μL of substrate (acetylthiocholine iodide). Three different concentrations of inhibitors were added to the assay solution and pre-incubated for 15 min at 37°C with the *Ee*AChE followed by the addition of substrate in different concentrations. Kinetic characterization of the hydrolysis of substrate catalyzed by *Ee*AChE was done spectrometrically at 412 nm. The parallel control experiments were performed without inhibitor in the assay. The plots were assessed by a weighted least square analysis that assumed the variance of v to be a constant percentage of v for the entire data set. Slopes of these reciprocal plots were then plotted against the concentration of **TM-33** in a weighted analysis, and K_i was determined as the intercept on the negative *x*-axis.

4.2.3. Molecular modeling studies

Dock was employed to identify the potential binding of compound **TM-33** to BuChE and AChE. The crystal structure of *hu*BuChE (PDB ID: 4tpk) and *Tc*AChE (PDB ID: 1EVE) were obtained from the Protein Data Bank after removing the original inhibitors and water molecules.[23] The 3D Structure of **TM-33** was built and performed geometry optimization by molecular mechanics. Docking studies were performed using the AUTODOCK 4.2.6 program. By using Autodock Tools (ADT; version 1.5.6), polar hydrogen atoms were added to amino acid residues, and Gasteiger charges were assigned to all atoms of the enzyme. The resulting enzyme structure was used as an input for the AUTOGRID program. AUTOGRID performed

a pre-calculated atomic affinity grid maps for each atom type in the ligand, plus an electrostatics map and a separate desolvation map presented in the substrate molecule. Flexible ligand docking was performed for the compounds. Each docked system was performed by 100 runs of the AUTODOCK search by the Lamarckian genetic algorithm (LGA). Other than the referred parameters above, the other parameters were accepted as default. A cluster analysis was performed on the docking results using a root mean square (RMS) tolerance of 1.0 and the lowest energy conformation of the highest populated cluster was selected for analysis. Graphic manipulations and visualizations were done by Autodock Tools or Discovery Studio 2.5 software.

4.2.4. Recombinant human MAO-A and MAO-B inhibition studies.

Recombinant human MAO-A and MAO-B were purchased from Sigma-Aldrich and stored at -80 °C. Tested compounds were prepared in DMSO (2.5 mM) and diluted with potassium phosphate buffer (100 mM, pH 7.40, containing KCl 20.2 mM) to a final volume of 500 μL containing various concentrations of test compounds (0-100 μM) and kynuramine (45 μM for MAO-A and 30 μM for MAO-B). The reactions were initiated by the addition of the enzyme (7.5 μg/mL) and then incubated for 30 min at 37. Then 400 μL NaOH (2N) and 1000 μL water were added to terminated the enzymatic reactions and the mistures were centrifuged at 16000g for 10 min.[25] The concentrations of the generated 4-hydroxyquinoline were determined by measuring the fluorescence of the supernatant on a Varioskan Flash Multimode Reader (PerkinElmer) with excitation and emission wavelengths at 310 nm and 400 nm, respectively. IC_{50} values were calculated from sigmoidal dose-response curves (graphs of the initial rate of kynuramine oxidation versus the logarithm of inhibitor concentration). Each sigmoidal curve was constructed form six different compound concentrations spanning at least three orders of magnitude. Data analyses were carried out with GraphRad Prism 5 employing the one site competition model. IC_{50} values were determined in triplicate and expressed as mean ± SD.

4.2.5. *In vitro* blood–brain barrier permeation assay

The blood-brain barrier penetration of compounds was evaluated using the parallel artificial membrane permeation assay (PAMPA) described by Di *et al.*[28] Commercial

drugs were purchased from Sigma and Alfa Aesar. Porcine brain lipid (PBL) was obtained from Avanti Polar Lipids. The donor microplate (PVDF membrane, pore size 0.45 mm) and acceptor microplate were both from Millipore. The 96-well UV plate (COSTAR) was from Corning Incorporated. The acceptor 96-well microplate was filled with 350 μL of PBS/EtOH (70:30), and the filter membrane was impregnated with 4 μL of PBL in dodecane (20 mg/mL). Compounds were dissolved in DMSO at 5 mg/mL and diluted 50-fold in PBS/EtOH (70:30) to a final concentration of 100 μg/mL. Then 200 μL of the solution was added to the donor wells. The acceptor filter plate was carefully placed on the donor plate to form a sandwich, which was left undisturbed for 18 h at 25 °C. After incubation, the donor plate was carefully removed, and the concentration of compounds in the acceptor wells was determined using the Varioskan Flash Multimode Reader (Thermo Scientific). Every sample was analyzed at ten wavelengths in four wells and in at least three independent runs. Pe was calculated using the following expression: $P_e = \{-V_d V_a/[(V_d + V_a)At]\}\ln(1 - \text{drug}_{acceptor}/\text{drug}_{equilibrium})$, where V_d is the volume of donor well, V_a is the volume in the acceptor well, A is the filter area, t is the permeation time, drug acceptor is the absorbance obtained in the acceptor well, and drug equilibrium is the theoretical equilibrium absorbance. The results are given as the mean ± standard deviation. In the experiment, 11 quality control standards of known BBB permeability were included to validate the analysis set. A plot of the experimental data versus literature values gave a strong linear correlation, $P_e(\text{exp}) = 0.9163P_e(\text{bibl.}) - 0.2247$ ($R^2 = 0.9558$). From this equation and the limit established by Di *et al.* (P_e (bibl.) = 4.0×10^{-6} cm/s) for blood–brain barrier permeation, we concluded that compounds with a permeability greater than 3.44×10^{-6} cm/s could cross the blood–brain barrier.

Acknowledgments

This work was supported in part by the Scientific and Technological Project of Henan Provincial (162300410103), the Key Scientific Research Project of Colleges and Universities in Henan Province (17B350002), the Special Project of Nanyang Normal University (ZX2016017) and Nanyang Normal University (STP2016009).

References

1. Thies, W.; Bleiler, L. *Alzheimers Dement.*, **2013**, *9*, 208.
2. Alzheimer's Disease International. World Alzheimer Report 2015: The Global Impact of Dementia.
3. Herrmann, N.; Chau, S. A.; Kircanski, I.; Lanctot, K. L. *Drugs.* **2011**, *71*, 2031.
4. Mohamed, T.; Rao, P.P. *Eur. J. Med. Chem.* **2016**, *26*, 823-843.
5. Arai, T.; Ohno, A.; Kazunori, M.; Kakizawa, T.; Kuwata, H.; Ozawa, T.; Shibanuma, M.; Hara, S.; Ishida, S.; Kurihara, M.; Miyata, N.; Nakaqawa, H.; Fukuhara, K. *Bioorg. Med. Chem.* **2016,** *24*, 4138.
6. Querfurth, H. W.; LaFerla, F. M. *N. Engl. J. Med.* **2010**, *362*, 329.
7. Garcia-Alloza, M.; Gil-Bea, F. J.; Diez-Ariza, M.; Chen, C. P.; Francis, P. T.; Lasheras, B.; Ramirez, M. J. *Neuropsychologia.* **2005**, *43*, 442.
8. Terry AV, Jr.; Buccafusco, J. J.; Wilson, C. *Behav. Brain. Res.* **2008**, *195*, 30.
9. Dringenberg, H. C. *Behav. Brain. Res.* **2000**, *115*, 235.
10. Youdim, M. B.; Edmondson, D.; Tipton, K. F. *Nat. Rev. Neurosci.* **2006**, *7*, 295.
11. Riederer, P.; Youdim, M. B. *J. Neurochem.* **1986**, *46*, 1359.
12. Caraci, F.; Copani, A.; Nicoletti, F.; Drago, F. *Eur. J. Pharmacol.* **2010**, *626*, 64.
13. Riederer, P.; Danielczyk, W.; Grünblatt, E. *Neurotoxicology.* **2004**, *25*, 271.
14. Bolea, I.; Juárez-Jiménez, J.; de Los Ríos, C.; Chioua, M.; Pouplana, R.; Luque, F. J.; Unzeta, M.; Marco-Contelles, J.; Samadi, A. *J. Med. Chem.* **2011**, *54*, 8251.
15. Cavalli, A.; Bolognesi, M. L.; Minarini, A.; Rosini, M.; Tumiatti, V.; Recanatini, M.; Melchiorre, C. *J. Med. Chem.* **2008**, *51*, 347.
16. Agis-Torres, A.; Sölhuber, M.; Fernandez, M.; Sanchez-Montero, J. M. *Curr. Neuropharmacol.* **2014**, *12*, 2.
17. Bajda, M.; Guzior, N.; Ignasik, M.; Malawska, B. *Curr. Med. Chem.* **2011**, *18*, 4949.
18. Li, X.; Wang, H.; Lu, Z.; Zheng, X.; Ni, W.; Zhu, J.; Fu, Y.; Lian, F.; Zhang, N. Li, J.; Zhang, H.; Mao, F. *J. Med. Chem.* **2016**, *22*, 8326.
19. Wang, Z.; Wang, Y.; Wang, B.; Li, W.; Huang, L. Li, X. *J. Med. Chem.* **2015**, *58*,

8616.

20. Youdim, M. B. H.; Weinstock, M. *Cell. Mol. Neurobiol.* **2002**, *21*, 555.
21. Meiring, L.; Petzer, J. P.; Petzer, A. *Bioorg. Med. Chem. Lett.* **2013**, *23*, 5498.
22. Carradori, S.; Silvestri, R. *J. Med. Chem.* **2015**, *58*, 6717.
23. Sang, Z.; Qiang, X.; Li, Y.; Yuan, W.; Liu, Q.; Shi, Y.; Ang, W.; Luo, Y.; Tan, Z.; Deng, Y. *Eur. J. Med. Chem.* **2015**, *94*, 348.
24. Qiang, X.; Sang, Z.; Yuan, W.; Li, Y.; Liu, Q.; Bai, P.; Shi, Y.; Ang, W.; Tan, Z.; Deng, Y. *Eur. J. Med. Chem.* **2014**, *76*, 314.
25. Li, Y.; Qiang, X.; Luo, L.; Yang, X.; Xiao, G.; Liu, Q.; Ai, J.; Tan, Z.; Deng, Y. *Eur. J. Med. Chem.* **2016**, *126*, 762.
26. Pérez-Cruz, F.; Vazquez-Rodriguez, S.; Matos, M.J.; Herrera-Morales, A.; Villamena, F.A.; Das, A.; Gopalakrishnan, B.; Olea-Azar, C.; Santana, L.; Uriarte, E. *J. Med. Chem.* **2013,** *56*, 6136.
27. Lu, C.; Guo, Y.; Yan, J.; Luo, Z.; Luo, H.B.; Huang, L.; Li, X. *J. Med. Chem.* **2013**, *56*, 5843.
28. Di, L.; Kerns, E. H.; Fan, K.; McConnell, O. J.; Carter, G. T. *Eur. J. Med. Chem.* **2003,** *38*, 223.

Figures, Schemes, and Tables Legends

Figure 1. Design strategy for 3,4-dihydro-2(1*H*)-quinoline-*O*-alkylamine derivatives

Figure 2. Steady state inhibition by compound **TM-33** of the AChE hydrolysis of ACh. The plots show mixed-type AChE inhibition for compound **TM-33.**

Figure 3 (A) Representation of compound **TM-33** (green stick) interacting with residues in the binding site of *Tc*AChE (PDB code: 1EVE). (B) 3D docking model of compound **TM-33** (green stick) with *Tc*AChE.

Figure 4 (A) Representation of compound **TM-33** (green stick) interacting with residues in the binding site of *hu*BuChE (PDB code: 4tpk). (B) 3D docking model of compound **TM-33** (green stick) with *hu*BuChE.

Figure 5. Toxicity effects of **TM-33** on cell viability in human PC12 cells. Data are mean values SEM of three independent experiments.

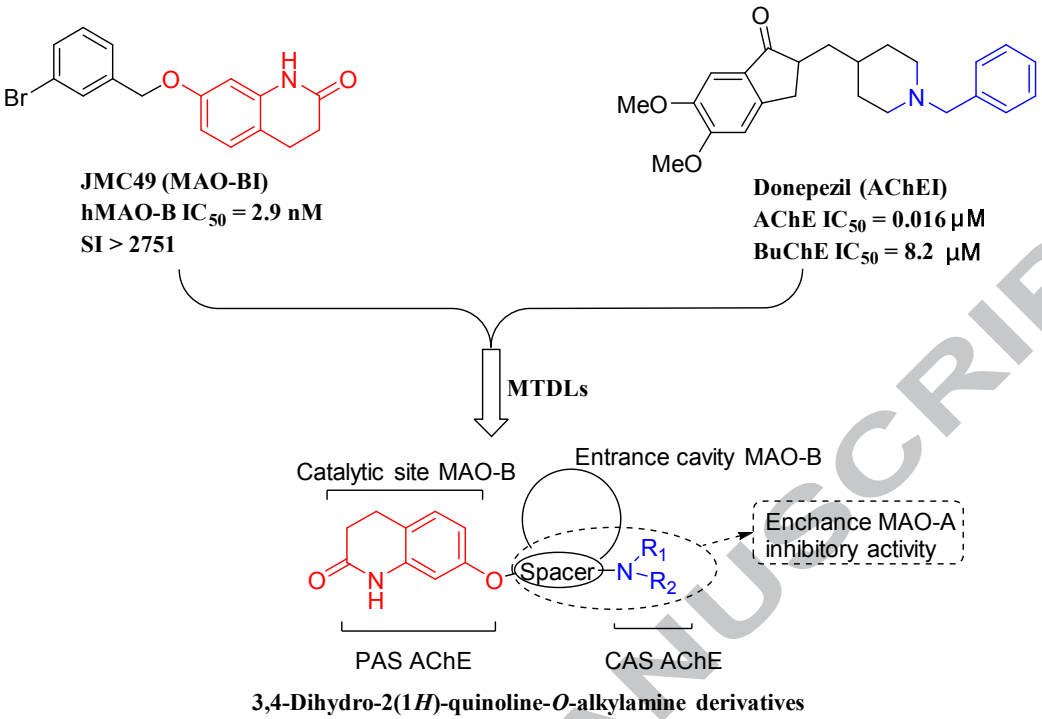

Figure 1.

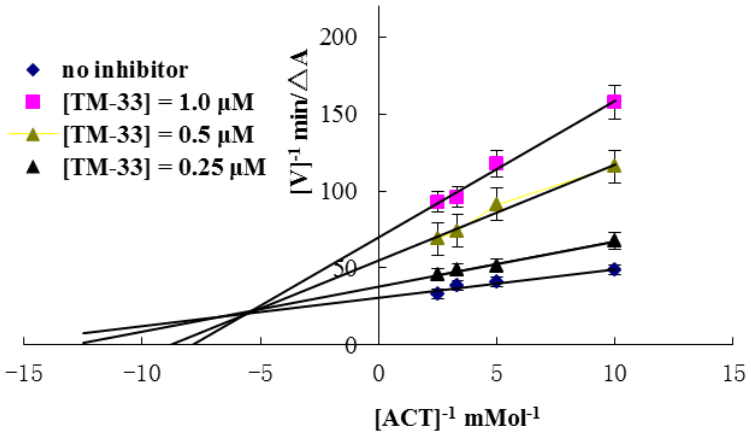

Figure 2.

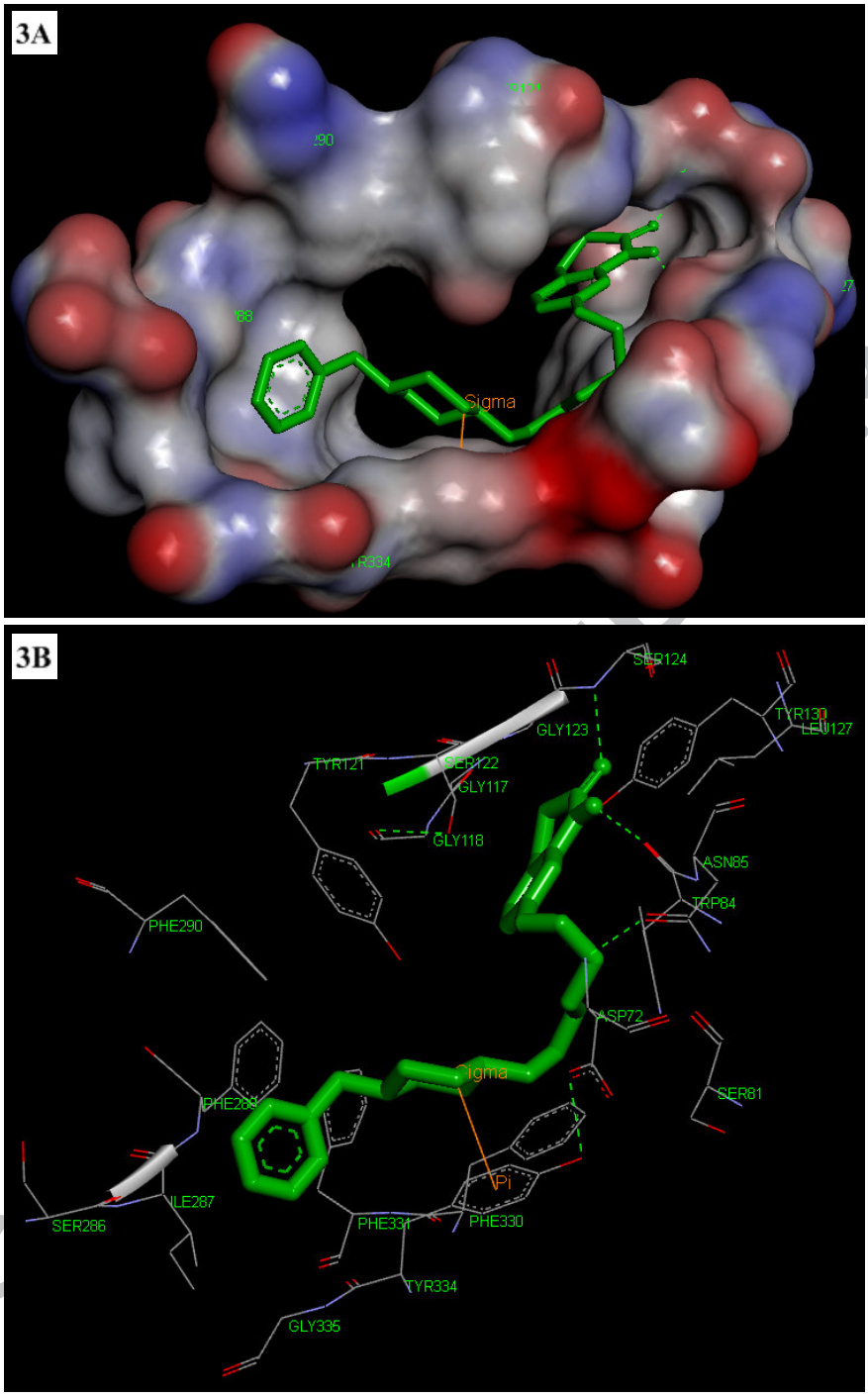

Figure 3

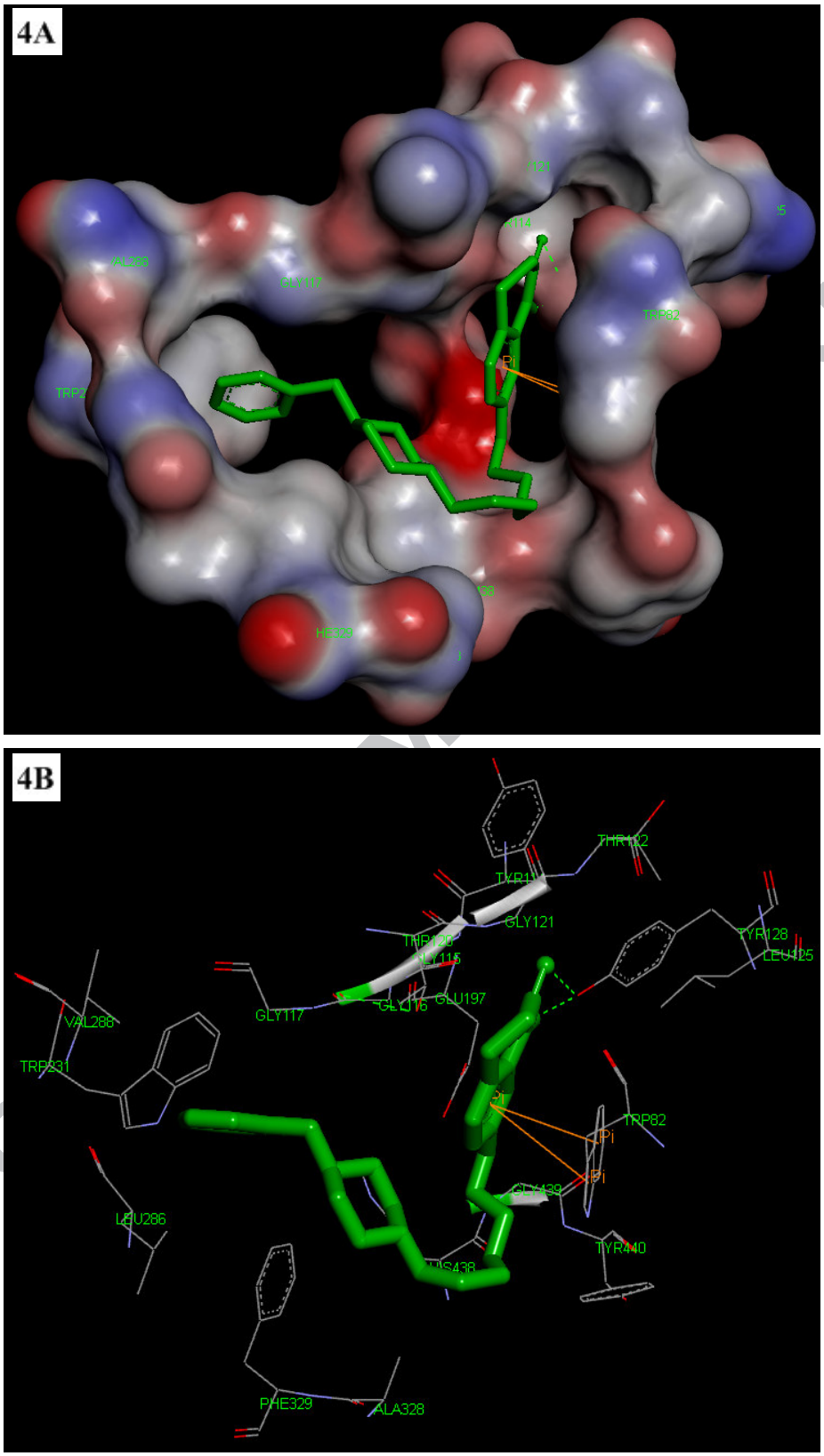

Figure 4

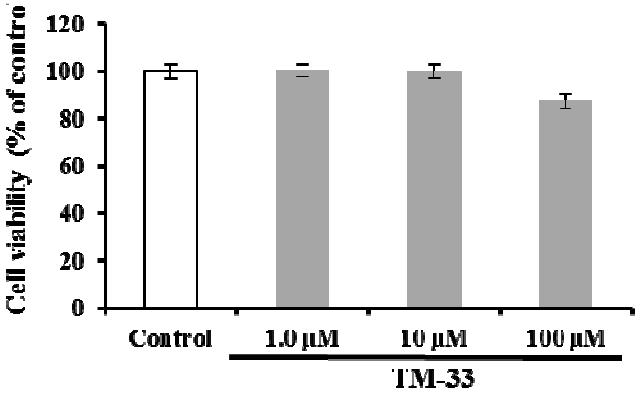

Figure 5

Scheme 1. Synthesis of 3,4-dihydro-2(1*H*)-quinoline-*O*-alkylamine derivatives (**TM-1~TM-31**). Reagents and conditions: (i) $Br(CH_2)_nBr$ (**2a~2d**), CH_3CN, reflux for 8-10 h. (ii) R_1R_2NH (**4a~4k**), K_2CO_3, CH_3CN, 65℃, for 6**-**10 h.

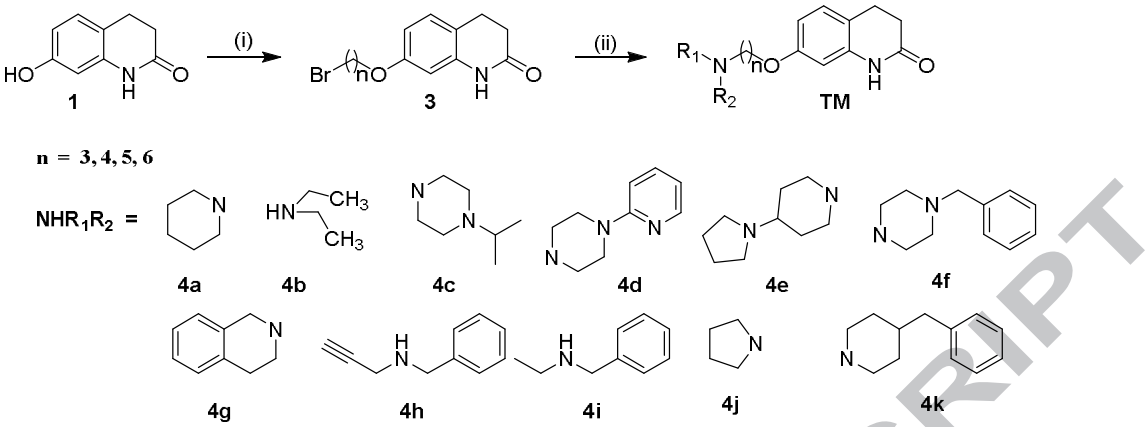

Scheme 1

Table 1 Inhibitory activities of AChE and BuChE by **1**, donepezil and **TM-1~TM-33**.

Table 2 MAO inhibitory activities of target compounds and reference compounds.

Table 3. Permeability P_e ($\times 10^{-6}$ cm/s) in the PAMPA-BBB assay of the selected compound **TM-33** and the predictive penetration in the CNS.

Table 4 The theoretical prediction of ADME properties of compound **TM-33**

Table 1

Comp.	n	NR_1R_2	IC_{50} (μM)[a]		SI[d]	IC_{50} (μM)[a]		SI[d]
			*Ee*AChE[b]	*Eq*BuChE[c]		*Rat*AChE[e]	*Rat*BuChE[f]	
TM-1	**3**	**4a**	**12.2±0.27**	**39.0±0.88**	**3.2**	**16.5±0.12**	**22.9±0.47**	**1.4**
TM-2	**3**	**4b**	**11.2±0.39**	**29.7±0.29**	**2.7**	**19.2±0.32**	**20.5±0.43**	**1.1**
TM-3	**3**	**4c**	**6.2±0.04**	**20.0±0.18**	**3.3**	**14.0±0.19**	**10.2±0.10**	**0.7**
TM-4	**3**	**4d**	**9.6±0.11**	**14.4±0.52**	**1.5**	**20.0±0.25**	**39.0±0.76**	**2.0**
TM-5	**3**	**4e**	**5.8±0.02**	**39.6±0.72**	**6.9**	**16.0±0.11**	**21.5±0.21**	**1.3**
TM-6	**3**	**4f**	**1.3±0.01**	**19.4±0.38**	**14.9**	**12.6±0.09**	**34.2±0.48**	**2.7**
TM-7	**3**	**4g**	**13.3±0.31**	**5.5±0.07**	**0.4**	**15.5±0.13**	**12.6±0.16**	**0.8**
TM-8	**3**	**4h**	**23.5±0.43**	**29.5±0.21**	**1.3**	**26.0±0.68**	**30.3±0.44**	**1.2**
TM-9	**4**	**4a**	**11.8±0.07**	**15.7±0.31**	**1.3**	**11.6±0.29**	**22.8±0.17**	**2.0**
TM-10	**4**	**4b**	**5.1±0.02**	**7.7±0.06**	**1.5**	**14.5±0.22**	**9.5±0.02**	**0.7**
TM-11	**4**	**4c**	**1.0±0.01**	**4.5±0.05**	**4.4**	**3.6±0.01**	**3.7±0.01**	**1.0**
TM-12	**4**	**4d**	**13.8±0.13**	**8.4±0.03**	**0.6**	**21.0±0.81**	**40.0±0.68**	**1.9**
TM-13	**4**	**4f**	**6.0±0.03**	**10.7±0.28**	**1.8**	**13.7±0.57**	**31.6±0.54**	**2.3**
TM-14	**4**	**4g**	**10.1±0.07**	**3.8±0.02**	**0.4**	**18.2±0.23**	**12.4±0.08**	**0.7**
TM-15	**4**	**4h**	**21.4±0.14**	**19.1±0.46**	**0.9**	**23.3±0.17**	**32.1±0.38**	**1.4**
TM-16	**5**	**4a**	**12.8±0.12**	**32.8±0.29**	**2.6**	**8.4±0.04**	**31.4±0.53**	**3.8**
TM-17	**5**	**4b**	**8.2±0.05**	**21.9±0.38**	**2.7**	**34.1±0.74**	**14.7±0.23**	**0.4**
TM-18	**5**	**4c**	**0.9±0.001**	**3.2±0.22**	**3.5**	**3.2±0.03**	**2.7±0.03**	**0.9**
TM-19	**5**	**4d**	**15.6±0.08**	**6.2±0.06**	**0.4**	**28.4±0.88**	**44.6±0.83**	**1.6**
TM-20	**5**	**4f**	**10.0±0.05**	**12.7±0.16**	**1.3**	**15.7±0.12**	**29.6±0.55**	**1.9**
TM-21	**5**	**4g**	**9.1±0.03**	**0.9±0.003**	**0.1**	**7.8±0.06**	**11.2±0.09**	**1.4**
TM-22	**5**	**4h**	**19.4±0.27**	**7.0±0.02**	**0.4**	**14.3±0.11**	**29.6±0.37**	**2.1**
TM-23	**6**	**4a**	**17.8±0.12**	**14.1±0.12**	**0.8**	**6.0±0.02**	**27.2±0.34**	**4.5**
TM-24	**6**	**4b**	**13.3±0.16**	**29.5±0.33**	**2.2**	**41.9±0.58**	**24.3±0.23**	**0.6**
TM-25	**6**	**4c**	**0.76±0.002**	**2.0±0.01**	**2.7**	**2.43±0.02**	**1.8±0.01**	**0.7**
TM-26	**6**	**4d**	**19.1±0.28**	**4.1±0.02**	**0.2**	**34.1±0.36**	**48.2±0.89**	**1.4**
TM-27	**6**	**4e**	**5.3±0.01**	**32.7±0.25**	**6.2**	**12.3±0.22**	**20.2±0.27**	**1.6**
TM-28	**6**	**4f**	**12.9±0.29**	**6.6±0.02**	**0.5**	**17.9±0.15**	**24.0±0.31**	**1.3**
TM-29	**6**	**4g**	**8.2±0.06**	**1.2±0.01**	**0.1**	**10.8±0.07**	**11.7±0.12**	**1.1**
TM-30	**6**	**4h**	**13.7±0.15**	**2.4±0.01**	**0.2**	**13.0±0.05**	**24.5±0.15**	**1.9**
TM-31	**6**	**4i**	**1.2±0.001**	**3.6±0.02**	**3.0**	**2.4±0.01**	**0.4±0.001**	**0.2**
TM-32	**6**	**4j**	**2.6±0.01**	**0.87±0.01**	**0.33**	**3.4±0.02**	**8.5±0.06**	**2.5**
TM-33	**6**	**4k**	**0.56±0.01**	**2.3±0.01**	**4.1**	**1.9±0.02**	**3.6±0.05**	**1.9**
1			**n.a.**[g]	**n.a.**[g]		**n.a.**[g]	**n.a.**[g]	
donepezil			**0.019±0.0003**	**4.76±0.02**	**251**	**0.037±0.0003**	**4.42±0.01**	**119**

[a] IC_{50} values represent the concentration of inhibitor required to decrease enzyme activity by 50% and are the mean of three independent experiments, each performed in triplicate (SD = standard deviation). [b] From *electrophorus electricusc*. [c] *Eq*BuChE from *equine serum*. [d] SI = selectivity index = IC_{50} (*Ee*AChE)/IC_{50} (*eq*BuChE). [e] From 5% rat cortex homogenate. [f] BuChE from rat serum. [g] n.a. = no active. Compounds defined "no active" means a percent inhibition of less than 5.0% at a concentration of 25μM in the assay conditions.

Table 2

Comp.	IC_{50} (μM)[a]		SI[d]
	MAO-A[b]	MAO-B[c]	
TM-1	13.1±0.15	6.2±0.03	0.5
TM-2	8.4±0.06	18.6±0.11	2.2
TM-3	9.4±0.04	26.1±0.21	2.8
TM-4	1.1±0.01	18.0±0.25	17.1
TM-5	9.6±0.03	19.2±0.13	2.0
TM-6	6.6±0.05	21.8±0.22	3.3
TM-7	8.6±0.02	18.8±0.18	2.2
TM-8	9.0±0.04	7.3±0.02	0.8
TM-9	9.5±0.03	6.4±0.01	0.7
TM-10	7.7±0.01	4.0±0.01	0.5
TM-11	14.3±0.15	7.6±0.03	0.5
TM-12	6.9±0.07	10.1±0.05	1.5
TM-13	7.4±0.02	9.4±0.01	1.3
TM-14	4.9±0.03	6.9±0.02	1.4
TM-15	9.3±0.02	9.1±0.02	1.0
TM-16	8.4±0.01	17.0±0.12	2.0
TM-17	11.4±0.02	8.5±0.01	0.7
TM-18	8.2±0.02	8.1±0.02	1.0
TM-19	13.0±0.03	20.3±0.22	1.6
TM-20	2.4±0.02	6.5±0.12	2.7
TM-21	4.6±0.01	5.9±0.01	1.3
TM-22	8.9±0.01	8.3±0.03	0.9
TM-23	9.4±0.02	31.7±0.36	3.4
TM-24	5.4±0.01	8.6±0.01	1.6
TM-25	6.8±0.02	24.9±0.27	3.7
TM-26	5.6±0.01	11.3±0.31	2.0
TM-27	6.2±0.03	18.3±0.35	3.0
TM-28	5.7±0.03	4.3±0.01	0.7
TM-29	3.4±0.01	4.4±0.02	1.3
TM-30	1.0±0.01	3.8±0.01	3.8
TM-31	1.2±0.01	1.7±0.01	1.5
TM-32	1.3±0.01	3.5±0.02	2.8
TM-33	0.3±0.001	1.4±0.01	4.7
iproniazid	3.18±0.03	1.78±0.01	0.56
clorgyline	0.0034±0.0001	5.02±0.02	1476
Rasagiline	2.13±0.01	0.086±0.003	0.04

[a] IC_{50} values represent the concentration of inhibitor required to decrease enzyme activity by 50% and are the mean of three independent experiments, each performed in triplicate (SD = standard deviation). [b] From recombinant human MAO-A. [c] From From recombinant human MAO-B. [d] SI = selectivity index = IC_{50} (MAO-B)/IC_{50} (MAO-A).

Table 3.

Compound[a]	P_e ($\times 10^{-6}$ cm/s)[b]	Prediction
TM-33	25.58 ± 0.67	CNS +

[a]Compound **TM-33** was dissolved in DMSO at 5 mg/mL and diluted with PBS/EtOH (70:30). The final concentration of the compound was 100 μg/mL.

[b] Values are expressed as the mean ± SD of three independent experiments.

Table 4

Comp.	Log *P*	MW	TPSA (Å^2)	n-ON	n-OHNH	volume (Å^3)
TM-33	4.63	378.52	41.57	4	1	371.74